Visible Light Degradation of 4-Nitrophenol Using Bi_2O_3/g-C_3N_4 Photocatalysts

Master of Philosophy
in
Environmental Sciences

By

HAJRA BATOOL
Registration No. 02312011002

DEPARTMENT OF ENVIRONMENTAL SCIENCES
FACULTY OF BIOLOGICAL SCIENCES
QUAID-I-AZAM UNIVERSITY
ISLAMABAD, PAKISTAN

2022

Visible Light Degradation of 4-Nitrophenol Using Bi_2O_3/g-C_3N_4 Photocatalysts

This work is submitted as a dissertation in partial fulfilment for the award of the degree of

Master of Philosophy
in
Environmental Sciences

By

HAJRA BATOOL
Registration No. 02312011002

DEPARTMENT OF ENVIRONMENTAL SCIENCES
FACULTY OF BIOLOGICAL SCIENCES
QUAID-I-AZAM UNIVERSITY
ISLAMABAD, PAKISTAN

2022

DEDICATION

Dear Ammi and Aboo,

As I stand at the threshold of completing my thesis, I am overwhelmed with a sense of gratitude and indebtedness to you both. Throughout my academic journey, you have been my constant pillars of support, guiding me with your unwavering love, encouragement, and belief in me.

Your selfless sacrifices, tireless efforts, and unconditional love have been the bedrock of my success. Your unwavering commitment to my education and future has never faltered, and for that, I will always be grateful.

This thesis is a culmination of years of hard work, determination, and perseverance, but it would never have been possible without your constant motivation and encouragement. I hope to make you proud by fulfilling all of my dreams.

As I dedicate this thesis to you both, I do so with all my heart, acknowledging the countless sacrifices you have made for me, and the unwavering love and support you have showered upon me. I hope this serves as a testament to your unwavering love and support.

Thank you, for everything you have done for me. I love you both more than words can ever express.

With love and gratitude,

Hajra Batool

Certificate of Approval

It is to certify that Ms. Hajra Batool (Reg. 02312011002) conducted the research work presented in this thesis, entitled **"Visible light driven degradation of 4-Nitrophenol using Bi2O3/g-C3N4 Photocatalysts"** under the supervision of **Dr. Abdullah Khan**. No part of this thesis has been submitted else for any other degree. This thesis is submitted to the Department of Environmental Sciences, in the partial fulfilment of the requirements for the degree of **Master of Philosophy (M.Phil.)** in the field of Environmental Sciences, Quaid-i-Azam University, Islamabad.

Hajra Batool (M.Phil. Scholar) _____

Supervisor:

Dr. Abdullah Khan _____

Assistant Professor

Department of Environmental Sciences

Quaid-i-Azam University, Islamabad, Pakistan

External Examiner:

_____

Chairman:

Dr. Sohail Yousaf _____

Department of Environmental Sciences

Quaid-i-Azam University, Islamabad

Date:

Declaration

I, **"Hajra Batool"** (Registration No. 02312011002) hereby declare that my M.Phil. thesis titled as **"Visible light driven degradation of 4-Nitrophenol using Bi_2O_3/g-C_3N_4 Photocatalysts"** is all my own effort done in Renewable Energy Advancement Lab, Department of Environmental Sciences Quaid-i-Azam University, Islamabad. All the investigations, findings, results, conclusions of this research have neither been previously presented anywhere nor published in any local or international forum.

Hajra Batool

Plagiarism Undertaking

I, **Hajra Batool**, hereby state that my M.Phil. Thesis titled as **"Visible light driven degradation of 4-Nitrophenol using Bi_2O_3/g-C_3N_4 Photocatalysts"** is solely my research work with no significant contribution from any other person. Small contribution/help whatever taken has been duly acknowledged and that complete thesis has been written by me.

I understand zero tolerance policy of the HEC and Quaid-i-Azam University, Islamabad, towards plagiarism. Therefore, I as an author of the above titled thesis declare that no portion of my thesis has been plagiarized and any material used as reference is properly referred/cited.

I undertake that if I am found guilty of any form of plagiarism in the above titled thesis even after the award of M.Phil. degree, the university reserves the right to withdraw/revoke my M.Phil. degree and that HEC and the university has the right to publish my name on the HEC/University website on which the names of students are placed who submitted plagiarism.

Hajra Batool

Acknowledgment

I am very grateful to **Allah Almighty**, who is most merciful and beneficent, who has blessed me with all of his blessings.

I wish to express my gratitude to **Chairperson** of the department of Environmental Sciences, Quaid-i-Azam University, Islamabad, who helped me with all the conditions necessary for the research.

I am really fortunate that I had the supervision of **Dr. Abdullah Khan**, Assistant Professor, Department of Environmental Sciences, Quaid-i-Azam University. His experties in the field of research is of immense value. His insightful feedback has always pushed me to sharpen my creativity and improved the quality of my work.

I would like to extend my gratitude to **Dr. Asima Siddiqa**, Senior Scientist, National Centre for Physics, Islamabad, for her encouragement, and professional guidance during my research.

I am also thankful to my friends **Muhammad Asim, Ahmad Khan, Liaba Gul,** and **Mehar wali** who helped me a lot in my research.

I would also like to appreciate the efforts of my siblings. Without their motivation and help, I believe I would not have been able to complete my work.

Completing this document was a challenge which I could not have finished without the moral support and encouragement of my all lab fellows (Renewable Energy Advancement Lab). Thank you all of you, for being so co-cooperative and supportive whenever I needed your help and guidance, be assured that Allah will bless you all for the contributions you made.

Hajra Batool

List of Acronyms

GHGs	Green House Gases
PL	Photoluminescence
UV-Vis	Ultraviolet Visible
XRD	X-Ray Diffraction
IPCC	Intergovernmental Panel on Climate Change
APIs	Active Pharmaceutical Ingredients
AOPs	Advance Oxidation Processes
CDDEP	Centre for Disease Dynamics and Policy
DDD	Defined Daily Doses
WWTP	Wastewater Treatment Plant
USEPA	United States Environmental Protection Agency
CCL	Contaminating Candidate List
CB	Conduction Band
VB	Valance Band
EMR	Electromagnetic Radiation
eV	Electron Volte
SEM	Scanning Electron Microscopy
TEM	Transmission Electron Microscopy
PZC	Point of Zero Charge
Ppm	Pert per million
Eg	Bandgap Energy

Table of Contents

List of Figures

LIST OF TABLES

Highlights:

- 4-Nitrophenol being a priority pollutant is toxic for both humans and animals
- The present work investigate the complete degradation of 4-Nitrophenol under simulated solar light
- The photocatalyst exhibited a much higher activity than pure g-C_3N_4 and Bi_2O_3
- Co-Bi_2O_3/g-C_3N_4 exhibited higher photocatalytic activity than 2.5% Bi_2O_3/g-C_3N_4 heterojunction

Graphical Abstract

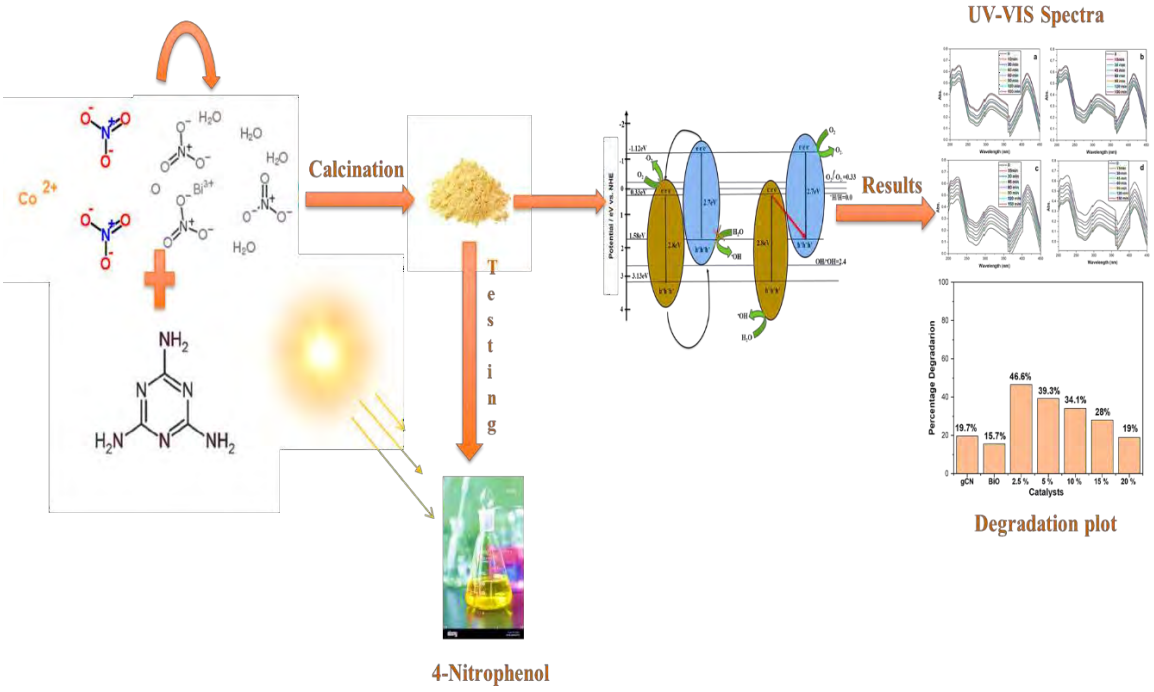

ABSTRACT

Cobalt doped bismuth oxide with graphitic carbon nitride has been synthesized using thermal method. As prepared heterojunction materials were characterized with various techniques such as UV-DRS, Scanning electron microscopy (SEM), Photoluminiscece (PL) and X-Ray Diaffraction (XRD). The Co-Bi_2O_3/g-C_3N_4 heterojunction was tested as a visible light active catalyst for degradation of 4-Nitrophenol. In comparison to pure g-C_3N_4 and Bi_2O_3, Co-Bi_2O_3/g- C_3N_4 showed better degradation of 4-Nitrophenol. The obtained degradation ability of pure g-C_3N_4 was only 19 percent, whereas Co-Bi_2O_3/g-C_3N_4 improved degradation up to 61 %. The influence of light, catalyst amount and pH on the photocatalytic activity will also be investigated. While testing the catalyst in dark reactions a negligible adsorption of <10% confirms that degradation mainly occurs in visible light. This workprovides an example to explore the role of other visible light active photocatalysts for the degradation of organic contaminants in water.

1. INTRODUCTION

For the last few decades, research has focused on determining the negative effects of global warming or the uncontrolled growth of greenhouse gases on our daily life. This anthropogenic climatic state has detrimental effects for human health and economic progress. [1]. It is urgent that we address the extreme use of fossil fuels immediately and create new regulations to mitigate global warming. Specifically, the investigations demonstrated that environmental conditions, food production, and availability to water are all severely impacted, causing some damage. It is likely to worsen in the future years, climate change has been linked to an increase in the incidence of infectious diseases such as diarrhea, dengue fever, and malaria.. Since heatwaves and air pollution continue to rise as a result of several industrial reasons, including electricity generation, cardiovascular health has also come under scrutiny in addition to a variety of respiratory problems [2]. Attempting to switch from using fossil fuels to using renewable energy is difficult. Laboratory and industrial studies have shown that it is more difficult than previously thought to strike a good balance between important factors like non-polluting or extremely low-polluting energy sources and energy efficiency. Thus, the main goal of finding a replacement was to reduce carbon dioxide emissions or other atmospheric pollutants associated with transport to the environment, such as nitrogen oxides, sulphur dioxide, PM10, and PM2.5, which contribute to air quality degradation and directly affect the health of people and other living species worldwide.[1]. Carbon dioxide contributes upto 80 per cent to global warming which is the most influential greenhouse gas (GHG). Global warming and greenhouse gases are directly associated with each other, when the concentration of GHGs increase global warming automatically rise. Renewable energy sources that can satisfy energy needs include solar energy, wind energy, hydropower, geothermal energy, and biomass. Solar energy is the most attractive energy source because the sun is an infinite source on which we can rely. It is the onlyway to reduce carbon emissions, though it has high capital cost at first time, but it is carbon free also. Earth receives 4.3 x 1020 J energy from sun which is more than the whole year energy demand

1.1 Introduction to environmental pollutants:

Environmental contaminants that are released into the environment as a result of human activities such as urbanization, mining, and industrialization have an impact on plants, animals, and human health. Toxic pollutants continue to affect living organisms in the environment through direct contact or bioaccumulation of chemicals from the environment. The harmful and toxic pollutants are easily transmitted to several environmental matrices, including surface and ground waters, air, and land.[3]

The release of harmful inorganic and organic pollutants from industry, agricultural operations, and municipal wastewater are the principal sources of water contamination, which is the greatest issue of the modern period. Pollutants present in bodies of water include heavy metals, herbicides, medicines, and dyes. At a specific level, the presence of these contaminants in drinking water is hazardous, providing a number of health concerns to humans. [4]

In order to satisfy the ever-increasing demand for clean water, several different methods have been tried up until this point in order to clean the water of such hazardous chemicals. Biological denitrification, ion exchange adsorption, reverse osmosis, chemical precipitation, photodegradation, catalytic reduction, electrodialysis, photocatalytic degradation [5] biodegradation, electrochemical degradation[6] have been employed.

1.2 Sources and routes of phenols in the environment:

Natural, industrial, residential, and agricultural activities all contribute to the release of phenolic chemicals into aquatic environments. The breakdown or decay of organic matter in water, the introduction of manmade pollutants, and agricultural runoff are all potential sources of these substances. [7] When these chemicals reach water, they have a propensity to mutate into new, perhaps more hazardous molecules. This transformation is usually brought on by their interaction with physical, chemical, biological, or microbial components of water. [8]

1.3 Anthropogenic Sources of Phenols are:

1. Industrial waste
2. Agricultural waste
3. Domestic waste
4. Municipal waste

1.4 Natural sources of Phenols:

1. Decomposition of organic matter
2. Synthesis by microorganisms
3. Synthesis by plants

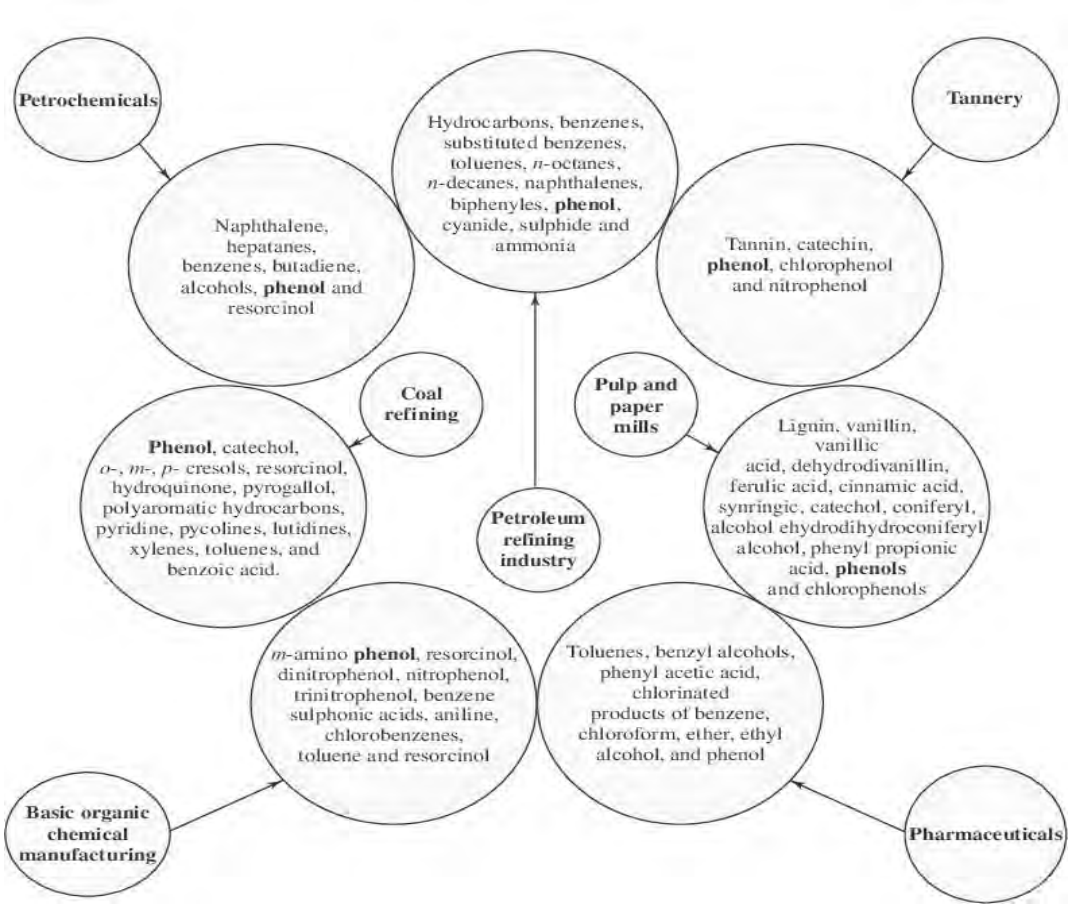

Figure 1.1: Sources of Phenol in Water [45]..

1.5 Selected pollutant 4-Nitrophenol:

4-Nitrophenol, also known as 4-NP, is a bio-refractory and hazardous pollutant that is capable of causing substantial damage to both human health and the environment. It has the potential to cause damage to the central nervous systems, livers, kidneys, and blood of both people and animals. Insecticides, herbicides, and other types of pesticides can all be manufactured using 4-NP and its derivatives. [9]

Phenols are commonly found as contaminants in soils and industrial effluent because they are widely utilized as intermediates in the production of dyes, insecticides, and pharmaceuticals. Due to their high toxicity and environmental persistence, they are classified as priority pollutants and are included in the US Environmental Protection Agency's (EPA) list of hazardous chemicals. Even at very low concentrations, the untreated release of phenols poses serious health risks to humans, animals, and aquatic systems. [10]

Despite the fact that 4-NP has several uses, it is a harmful contaminant. However, it's reduced form, 4-AP, is significantly less harmful and is actually employed as a raw material in the production of cosmetics and organic dye. [11]

Physio-chemical and biological oxidation are the standard approaches for treating industrial wastewater. (E.g. activated carbon adsorption, Nano filtration, and coagulation–flocculation). Due to 4-NP's great stability and water solubility, biological processes do not produce adequately effective results. The fundamental drawback of physical-chemical procedures is that they do not remove contamination; rather, they only shift it from one phase to another, resulting in secondary waste production and the need for additional treatments. [9]

Over the past two decades, advanced oxidation processes (AOPs) have shown promise as an effective method for removing pollutants from wastewater. Hydroxyl radicals that are extremely reactive and nonselective and are able tooxidize the majority of poisonous and dangerous organic compounds in industrial effluents[12].

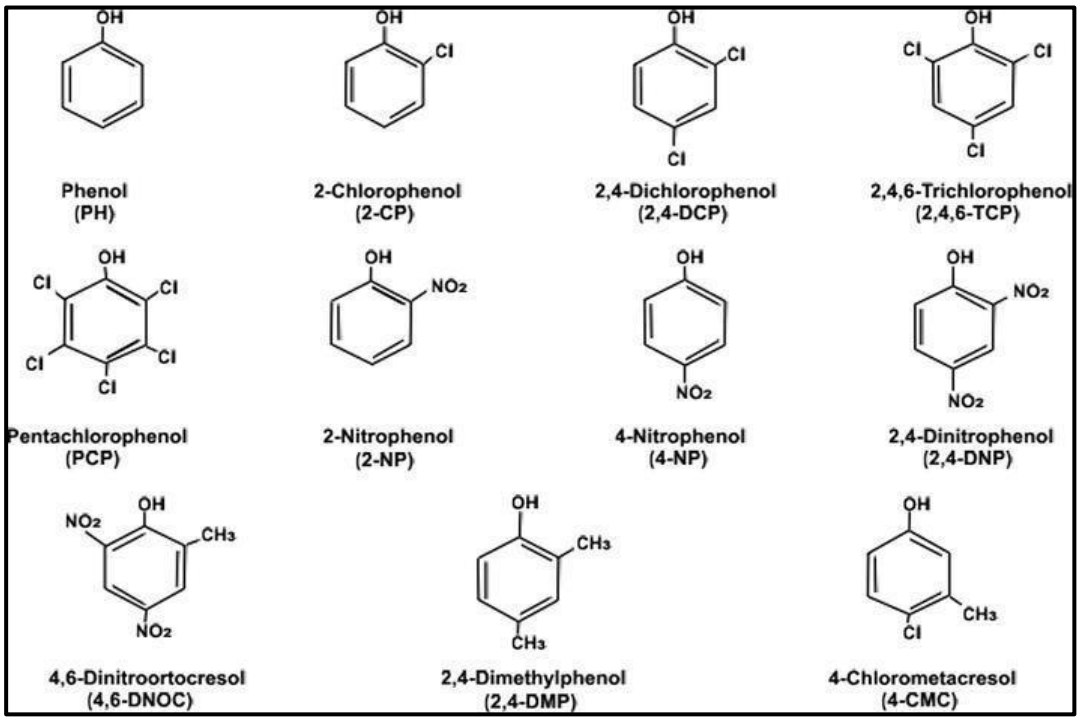

Figure 1.2: Phenolic compounds structures considered priority contaminants by US EPA[13]

1.6 Toxic effects of phenolic compounds on humans:

The vast majority of phenolic compounds are quickly absorbed through the gastrointestinal tracts of humans and can easily penetrate human skin when absorbed through the dermis. After entering the body, these substances go through the metabolic process and are converted into a variety of reactive intermediate forms, most notably quinone moieties. These moieties are able to readily form covalent bonds with proteins and, as a result, have the potential to be harmful to human beings. [14]. A wide variety of phenolic compounds, including chlorophenols, aminophenols, chlorocatechols, nitrophenols, methylphenols, and others, have been found to be harmful to human health.

The consumption of liquids containing a high concentration of phenol, such as drinking water, results in digestive issues, muscle tremors, and trouble walking. When utilizing products with a high phenol concentration, exposure to excessive quantities of phenol can cause damage to the heart, kidneys, and liver, as well as blisters and burns on exposed skin.

1.7 Wastewater treatment methods:

To prevent possible contamination of humans and aquatic organisms by these toxic chemicals, it is imperative that phenolic compounds be recovered from the aquatic environment. Utilizing the right technology to remove these substances effectively would not only solve waste disposal issues and difficulties related to potential harm from pollutants, but will also enable the achievement of value-added 426 Phenolic Substances- Natural Sources, Importance and Applications phenolic compounds as by-products. The strategies used to successfully remove phenolic compounds from wastewater before their final release into water bodies are covered in this section.[7]

1.7.1 Biological methods

In biological wastewater treatment methods various microbes and enzymes are used to remove different kinds of toxicity from water.

1.7.2 Chemical methods

Using different types of chemicals to clean wastewater for the purpose of drinking, following well known method are observed.

- Ozonation
- Chlorination
- Precipitation
- Chemical oxidation

1.7.3 Traditional physical methods

- Adsorption
- Ultrafiltration
- Reverse osmosis

1.8 Conventional Processes for the Removal of Phenolic Compounds:

In addition to these conventional treatments, there are also emerging technologies that show promise in removing phenolic compounds from wastewater and other sources. One such technology is advanced oxidation processes (AOPs), which use hydroxyl radicals to oxidize and degrade organic pollutants. Other promising techniques include membrane filtration, ion exchange, and bioremediation, which involve using natural microorganisms to break down and remove phenolic compounds. Overall, there are a variety of approaches available for removing phenolic compounds, and the most appropriate method will depend on factors such as the specific compounds present, the concentration of pollutants, and the desired level of treatment.

Table 1.1: Conventional Waste water treatment Methods

Process name	Component
Adsorption	The economics and recycling of the necessary secondary material, adsorbent, make adsorption an attractive option for removing phenols from water at low to high concentrations.
Membrane processes	Water and wastewater organic pollutants are removed via membrane processes. The elimination of phenolic chemicals is presently the subject of research into this technique. Applications for separation membranes include purifying procedures and nanotechnology.
Reverse osmosis and Nano filtration	To extract dissolved particles, notably ions, from aqueous solutions, RO is a membrane-based demineralization process. Contrarily, the removal of organic contaminants, inorganic salts, color, and hardness from aqueous solutions is commonly accomplished using nanofiltration (NF).
Electrochemical oxidation	Another method of phenol destruction that does not involve the use of chemicals is electrochemical oxidation. This method is classified as either direct or indirect oxidation.
Biological treatment	The most common technique for getting rid of phenols in water is biological treatment. The process converts phenolic solutions into simple end products at a cheap cost and with little maintenance..

1.9 Advanced Oxidation Process

It is generally agreed that advanced oxidation processes, sometimes known as AOPs, are among the most effective technologies for removing organic pollutants from water. [15] In 1980, AOPs were first proposed for the filtration of drinking water. Thereafter, substantial study was conducted on them as oxidizing treatments for various wastewaters. Recovered effluents can be made through the use of advanced oxidation processes (AOPs), which are oxidation processes that generate large amounts of ROS like hydroxyl radicals (HO). The redox potential of HO radicals is quite high (2.8 eV), and they are nonselective. [16] Hydrogen abstraction, radical combination or addition, electron transfer, and oxidation are the four mechanisms by which they can attack organic compounds. Wastewater including pesticides, phenols, chlorophenols, and dyes has been successfully treated using a variety of AOPs (e.g., ultrasonic, Fenton, ozone, and UV radiation)[17]. These AOPs have shown promise in breaking down a wide range of refractory pollutants, and their gentle reaction conditions are an added bonus.

1.9.1 Photocatalysis:

Photocatalysis is a process that initiates or speeds up a reaction using light as a source of energy. The energy can be UV or visible light. A lot of attention is being paid on photocatalysis due to its applications and uses in different fields of science. This process is also being widely tested and used in treatment of water and removal of organic and inorganic wastes from the water. This process is also being used in the removal of organic pollutants like phenols [18]

Photocatalysis offer following benefits over conventional process:

i. Renewable, pollution free solar energy is used.
ii. In situ treatment is possible.
iii. Offers less burden on economy compared to other treatment methods.
iv. Minimum secondary waste is generated.
v. Photocatalysts can be reused again many times.
vi. There is no need to install separate large area occupying plants for wastewater treatment.

These advantages make photocatalysis a viable and environmental friendly, as well as economic friendly option to opt for treatment of organic pollutants from wastewater on

large scale.

1.9.2 Principle of photo catalysis

Electrons are excited and jump to the conduction band when light hits a semiconductor's surface, leaving a hole in the valence band. **(Figure 1.3)**

$$\text{Semiconductor} + \text{Light} \rightarrow e^- + h^+$$

Where e^- represents the electron in conduction band and h^+ represents the hole in the valence band. Now these two bodies get into a redox reaction where other species are already present on catalyst surface. Hole h+ can react with a surface-bound H_2O molecule to produce OH, while hole e- can react with O_2 to produce superoxide radical anion of oxygen O_2-.

$$H_2O + h^+ \rightarrow OH^{\cdot} + H^+$$

$$O_2 + e^- \rightarrow O_2^{-\cdot}$$

The resulting hydroxide radicals and oxygen radical anion can react with organic and inorganic pollutants. [19]

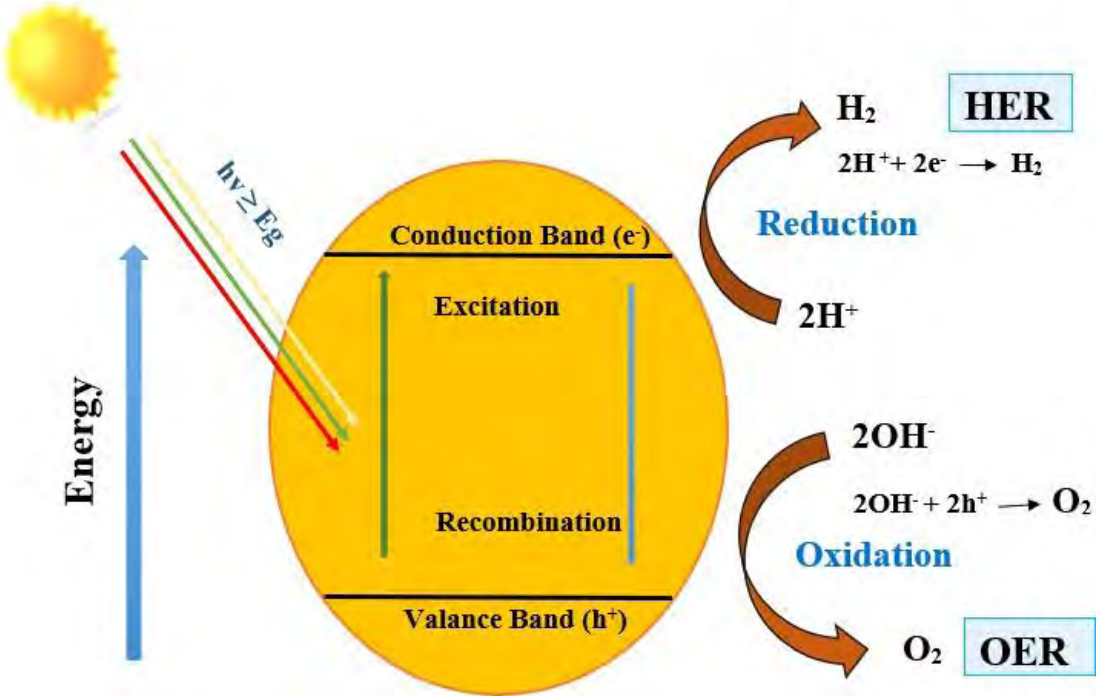

Figure 1.3: Schematics of principle of Photo-catalysis.

1.10 Strategies to improve the photocatalytic activity of material

1.10.1 Doping:

Since Bi_2O_3 has a larger band gap, UV radiation must be used for photodegradation rather than sunshine, which is a renewable resource. This feature, that the band gap can be tuned by doping with metal ions, is crucial. Typically, metal ion doping modifies the electronic structure of the host material, resulting in dramatic changes in its optical, electrical, and magnetic properties. Doping is a widely utilized technique for boosting photocatalytic performance. The greater charge separation efficiency of doped Bi_2O_3 is a possible explanation for its increased catalytic activity. [20].

Coupled with this, cobalt doping increases the photocatalytic activity of Bi_2O_3 and extends the photo response to the visible spectrum.[20] Cd doped Bi2O3, Au nanoparticles modified Bi2O3 and Ag doped Bi2O3 have been reported [21]

1.10.2 Heterojunction:

The photocatalytic activity of Bi_2O_3 is constrained by the rapid recombination and photocorrosion of photogenerated charge carriers, which is a limitation on the photocatalytic potential of Bi_2O_3. In order to solve these issues, heterojunction photocatalysts have been prepared in order to boost the photocatalytic activity of Bi_2O_3. Some examples of these heterojunction photocatalysts include $Bi_2O_3/BaTiO_3$, Bi_2O_3/TiO_2, and Bi_2O_3/Bi_2WO_6, amongst others. [22] Different types of heterojunctions have been documented in literature depending uponband gap alignment of integrated material.

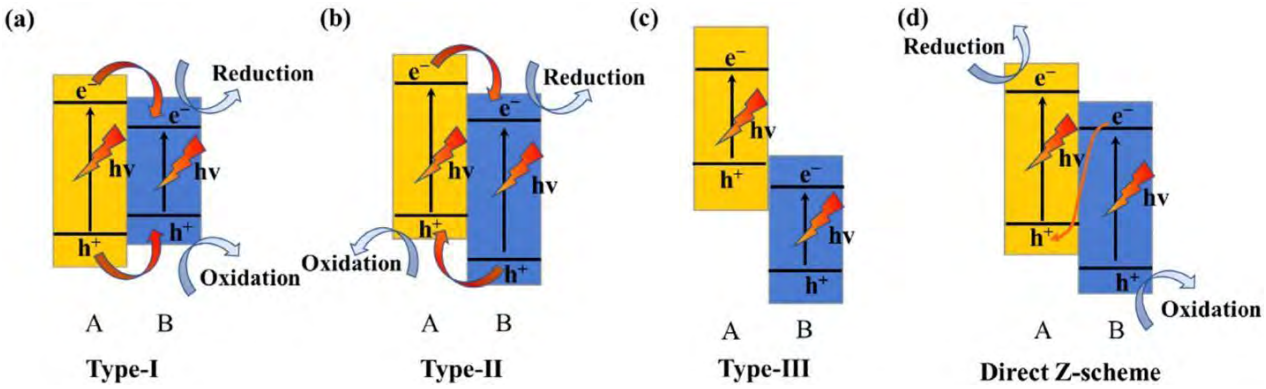

Figure 1.4: Types of heterojunctions [21].

There are three types of heterojunctions based on the relative positions of the valence

and conduction bands of the two materials involved.

In Type I heterojunctions, both the valence and conduction bands of one material are located inside the bandgap of the second material.

In Type II heterojunctions, the valence and conduction bands of one material are higher than the valence and conduction bands of the second material.

In Type III heterojunctions, the energy position of the bandgap of one material is greater than that of the second material.

Each type of heterojunction has its own unique properties

1.10.3 Proposed System:

The material known as graphite C_3N_4 (g-C_3N_4) has become a topic of significant importance in the field of photocatalysis due to several advantageous features. These include its non-toxic nature, low cost, and the ease with which it can be synthesized through the heating of melamine, dicyandiamide, and urea. The approximate band gap of g-C_3N_4 is 2.7 eV, allowing it to effectively absorb visible light up to 460 nm in wavelength.[23] However, its photocatalytic activity is low because of the rapid recombination of electron-hole pairs generated by light.

There are six different polymorphs of the chemically stable metal oxide bismuth oxide (Bi_2O_3). These polymorphs are designated a, b, c, d, x, and e. [24]. However, photocorrosion and the rapid recombination of photogenerated charge carriers limit the photocatalytic activity of Bi_2O_3. The heterojunction has been designed to improve the photocatalytic performance of Bi_2O_3 [23] like Bi_2O_3/g-C_3N_4 and Co- Bi_2O_3/g-C_3N_4

1.10.4 Limitations of Bi_2O_3

As a result of the greater band gap of Bi2O3 (2-3.9 eV), which necessitates the employment of UV light for photo-degradation, sunlight is unable to be used. Doping with metal ions is an effective method for customizing the band gap, which is essential because of its importance. In most cases, metal ion doping causes dramatic alterations in the optical, electrical, and magnetic properties of the host material by altering the structure of its electronic molecules. [20].

1.10.5 Transport process of photo excited carriers:

The heterojunction photocatalyst Bi_2O_3/g-C_3N_4 is generated when Bi_2O_3 and g-C_3N_4 are joined.

The standard electron-hole separation mechanism for many composite photocatalysts, as shown in Fig. 1.5(a), involves the movement of charge carriers in Bi_2O_3/g-C_3N_4, causing electrons in the Conduction band of g-C_3N_4 to move to the CB of Bi_2O_3, and holes in the Valence Band of Bi_2O_3 to move to the VB of g-C_3N_4. However, this mechanism does not produce the reactive species necessary for high photocatalytic activity, such as •O_2, •OH, and h+. Research has shown that a different mechanism, as shown in Fig. 1.5(b), is responsible for producing these reactive species. In this mechanism, photoexcited electrons in the CB of Bi_2O_3 and photoexcited holes in the VB of g-C_3N_4 are quickly connected, producing a high concentration of active species. Additionally, the electron accumulation in the CB of g-C_3N_4 produces a higher negative potential, leading to the breakage of oxygen molecules into O_2, while the electron accumulation in the VB of Bi_2O_3 produces a higher positive potential, leading to the production of a lot of active OH radicals. As a result, the Bi_2O_3/g-C_3N_4 system exhibits significantly higher photocatalytic activity. [23].

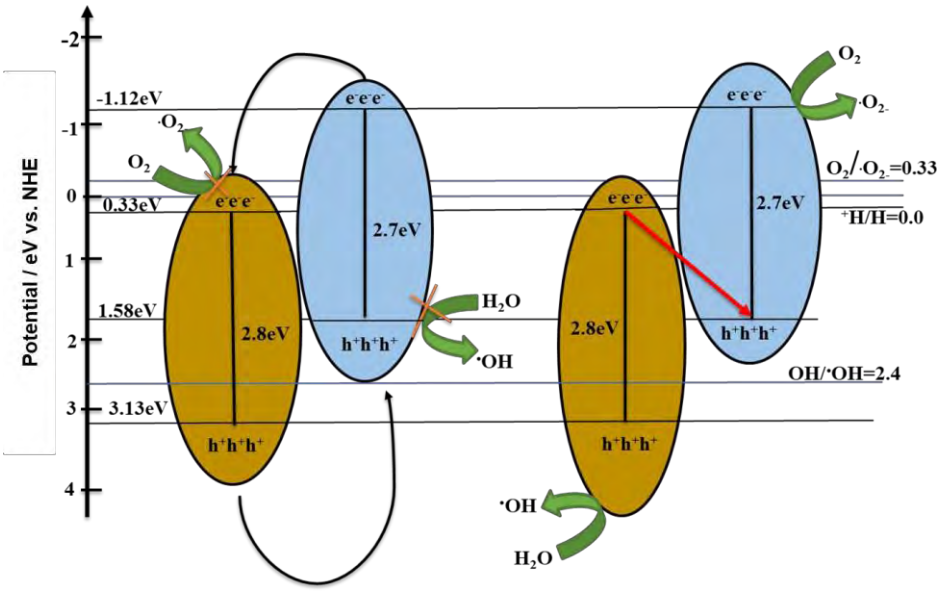

Figure 1.5: Schematic diagram of photo-exited electron-hole separation process [23].

1.11 Problem statement:

4-nitrophenol is a highly toxic organic pollutant that poses a significant threat to human health and the environment. This compound is commonly found in industrial wastewater, agricultural runoff, and other sources, and is resistant to conventional treatment methods. Exposure to 4-nitrophenol can cause a range of health problems, including liver and kidney damage, neurological disorders, and even cancer. Additionally, the persistence of 4-nitrophenol in the environment can lead to long-term ecological damage, including the destruction of aquatic ecosystems and the contamination of soil and groundwater. The urgent need for effective and sustainable solutions for the removal of 4-nitrophenol from water and other environmental sources underscores the importance of developing innovative approaches that can provide efficient and cost-effective treatment options while minimizing the risk to human health and the environment. Therefore, nanotechnology is considered as a viable option for the complete degradation of 4-Nitrophenol. Different photoactive catalysts have been synthesized and tested for the degradation of 4NP. Different problems have beenwith these catalysts either they were UV active or give limited degradation in solar light. These catalysts are expensive, rarely available, and are not eco-friendly. These problems can be overcome by making these catalysts cheap, non-toxic, removable, reusable, and efficient in solar light. Co- Bi_2O_3/ gC_3N_4 is a novel solar catalyst that has never been synthesized and tested before for the degradation of 4-Nitrophenol.

1.12 Aims and objectives of the study

The main objective of this study is to synthesize an efficient photoactive system of Bi_2O_3/ gC_3N_4 to degrade organic pollutant under visible light.

To accomplish this goal, following aims are also considered.

1) Synthesis of efficient and stable heterojunction of Bi_2O_3/ gC_3N_4
2) 3% doping of Cobalt to improve charge transfer behavior of Bi_2O_3.
3) Synthesizing different ratios of $Bi_2O_3$and gC_3N_4 to check optimum level of combination.
4) Degradation of most prevalent and persistent phenol in wastewater.
5) Study effects of pH, catalyst amount, and initial pollutant concentration on the degradation of 4-Nitrophenol

2. MATERIALS AND METHODS

This chapter includes the descriptions of materials that are used in the synthesis of proposed system that is Co- Bi_2O_3/ gC_3N_4 heterojunction. It also includes methods adapted for synthesis and for testing. Four catalyst are prepared. These are:

1) Bi_2O_3
2) g-C_3N_4
3) Bi_2O_3/ g-C_3N_4
4) Co- Bi_2O_3/ g-C_3N_4

Same precursor materials were used in all synthesis of all samples and same method was applied to carry out efficient synthesis.

2.1 Materials essential for synthesis

Melamine (99%, Sigma), $Bi(NO_3)_3$. $5H_2O$ (> 99.99%, Sigma) and Cobalt nitrate were used without further purification.

2.2 Synthesis methodology for Bi_2O_3

Nanocrystals of bismuth oxide were produced by subjecting bismuth nitrate pentahydrate to a solid state decomposition reaction at a temperature of 500 degrees Celsius for four hours. The product was then dried for a total of six hours at a temperature of 80 degrees Celsius after being rinsed with distilled water.s.

2.3 Synthesis of g-C_3N_4:

For the manufacturing of g-C3N4 thermal polymerization of melamine in muffle furnace at atmospheric pressure method was adopted [25]. In this technique, 10 gram melamine powder was placed in an aluminum foil-wrapped crucible and heated at 550 °C for 4 hours at an increasing rate of 3 °C before being allowed to cool down gradually at ambient temperature.

The yellow material collected was rinsed three times with D.I water and centrifuged at 4000 rpm. The yellow material was then dried in an oven at 80 °C until totally dry, after which it was crushed and stored in falcon tubes for subsequent use.

2.4 Synthesis of Bi_2O_3/ g-C_3N_4

The typical preparation of Bi_2O_3/ gC_3N_4 composites was as follows:

In a mortar and pestle, a range of bismuth oxide concentrations and graphitic carbon nitride concentrations were ground for 30 minutes. The final powder mixture was placed in a crucible with a lid and heated at 500°C in a muffle furnace at a rate of 20°C/min. The final Bi_2O_3/ gC_3N_4 Composites with various Bi_2O_3 contents were obtained. 2.5% Bi_2O_3/ gC_3N_4, 5% Bi_2O_3/ gC_3N_4, 10% Bi_2-O_3/ gC_3N_4, 15% Bi_2O_3/ gC_3N_4, and 20% Bi_2O_3/ gC_3N_4 were prepared by using this method

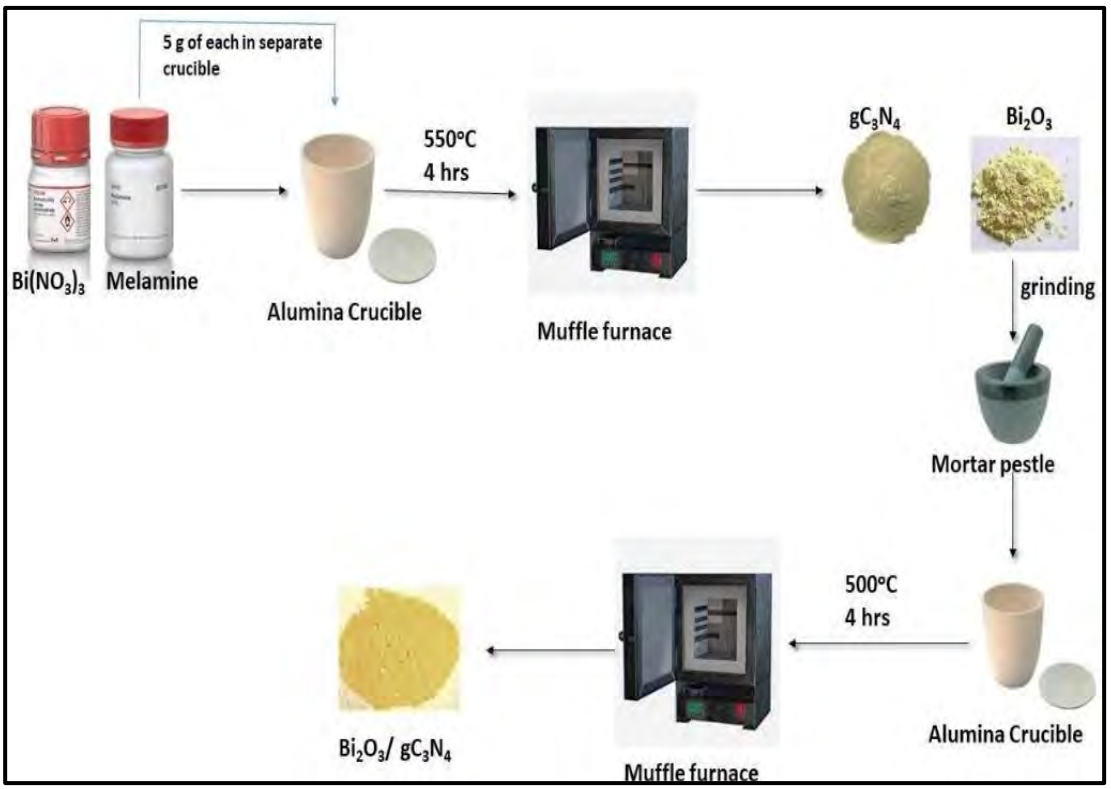

Figure 2.1: Schematic representation of synthesis of Bi_2O_3/g-C_3N_4.

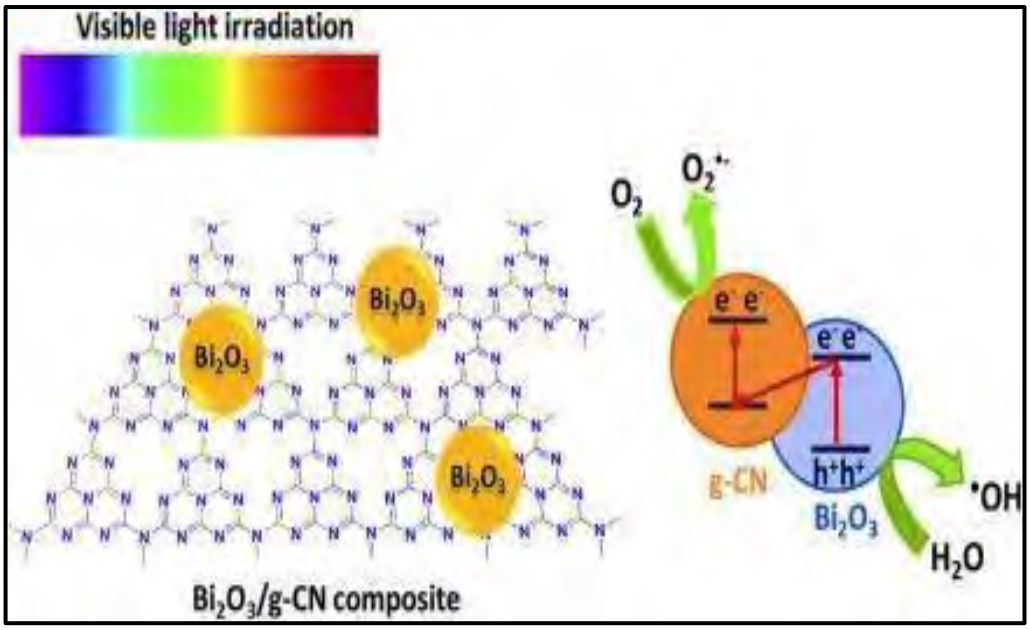

Figure 2.2: Pictorial representation of synthesis of Bi_2O_3/g-C_3N_4 composite.

2.5 Synthesis of Co-Bi_2O_3/ g-C_3N_4

To make 3% cobalt-doped bismuth oxide nano powders, we dissolved 1.0 M bismuth nitrate penta-hydrate in 50 mL deionized water and vigorously stirred the solution. Next, 0.15 g of cobalt that had been dissolved in 50 mL of deionized water was added. Under constant stirring, 0.1 M sodium hydroxide was added drop by drop to the solution. At 80°C, the resulting solution was stirred for four hours until a pale yellow precipitate formed. The precipitate was repeatedly washed with deionized water and then filtered. After drying the precipitate in a 100°C hot air oven for one hour, we annealed it at 500°C for four hours in a muffle furnace to obtain phase-pure cobalt-doped bismuth oxide nano powders. [20]. In order to make heterojunction, Cobalt doped bismuth oxide Nano powder was combined with graphitic carbon nitride in a suitable ratio in mortar and pestle. Grind this for 30 minutes. Put this in crucible and cover it with lid. The mixture was then heated at 500ºC for 4 hours at 20º per minute rise in muffle furnace. Yellowpowder will be obtained indicating the synthesis of Co-Bi_2O_3/ gC_3N_4.

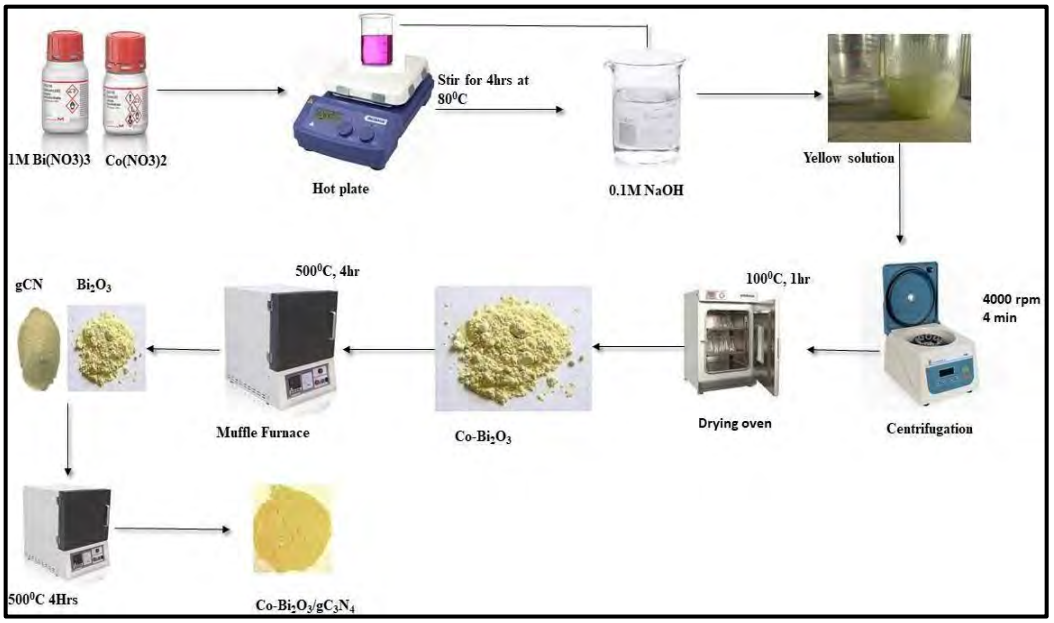

Figure 2.3: Schematic representation of synthesis of Co-Bi_2O_3/ g-C_3N_4.

2.6 Photocatalytic Experiment

In every experiment, prior to irradiation, 50 mL of a variable concentration 4-NP aqueous solution containing the needed amount of catalyst was swirled continuously for 30 minutes in the dark to achieve adsorption equilibrium. At that time, approximately 5 ml of sample was extracted using a syringe for examination to assess the adsorption capacity of the catalyst. Following this, the reaction mixture was agitated constantly under sunlight, and 5 ml aliquots were extracted at specified intervals up to 3 hours. To remove the photocatalyst, the aliquots were centrifuged at 4000 revolutions per minute for four minutes. The remaining 4-NP concentration in the filtered solution was quantified using a UV-Vis spectrophotometer to measure absorbance at λ max = 316 nm[26].

The degradation efficiency of 4-NP is calculated by the following equation;

$$\boldsymbol{Degradation\ Efficiency}\ \% = \left(\frac{\boldsymbol{C_0 - C}}{\boldsymbol{C_0}}\right)\ \boldsymbol{x\ 100}$$

where Co is the initial concentration of 4-Nitrophenol solution (mg/L), Ct is the concentration of 4-Nitrophenol after irradiation after selected time interval (mg/L)[20]

2.7 Characterization Techniques

This chapter will concentrate on the most widely used and effective techniques for characterizing nanoparticles[27]. The primary objective of this chapter is to provide a theoretical and practical description of the techniques used to characterize a wide variety of materials. The method's suitability, sample set-up, and expected outcomes will be discussed in detail. The molecular structure of photocatalyst is studied using several analytical tools, such as ultraviolet-visible spectroscopy, X-ray diffraction (XRD), scanning electron microscopy (SEM), and transmission electron microscopy (TEM).[28]

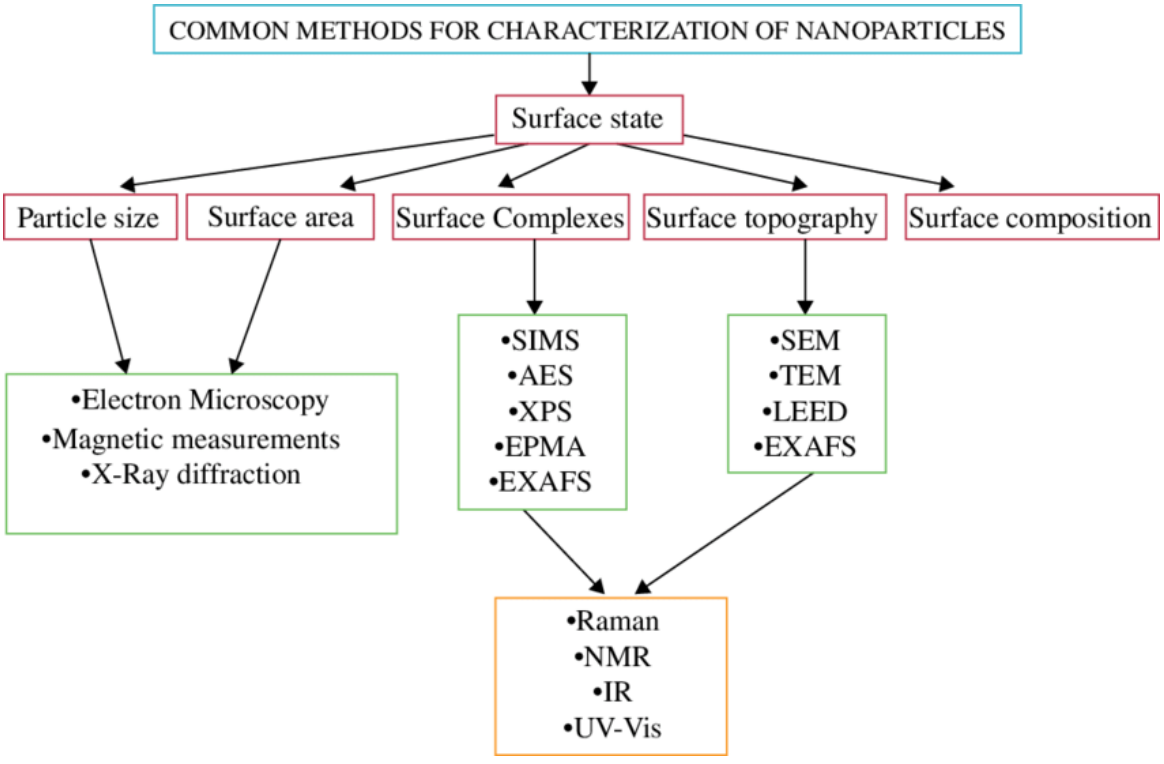

Figure 2.4: Some common characterization techniques for nanoparticles[29].

2.7.1 Photoluminescence (PL)

Photoluminescence spectroscopy, often known as PL, occurs when light energy, or photons, induce the emission of a photon from any substance. It is a noncontact, nondestructive method of material inspection.. Photoluminescence is a technique in which nanoparticles are illuminated with a light source. The results are recorded and plotted in the form of emission and absorption peaks.

Principle of PL

Photoexcitation occurs when excess energy of the striking radiation is imparted to the sample material. Electrons are excited to high energy levels, the excited states. The excited electrons gain their stable levels of energy, the ground state by releasing the absorbed photon of light and give an emission spectrum also known as photoluminescence. Photoluminescence is the energy difference between the ground states and the excited states[30]

The relationship between energy and wavelength is given by the equation $E\ (eV) = hc/\lambda$. Where h represents Plank's constant and c denotes the speed of light. Their valuesare collectively 1240. So we can rewrite the equation as $E(eV) = 1240/\lambda$[30]

Instrument and Working of Photoluminescence

Elements that are responsible for PL system to run and give results are as follows:

- Source of illumination
- Monochromators
- Gratings
- Slits and shutters
- Sample compartment
- Detectors

A continuous light source is used which falls on the two Monochromators i.e., an emission and an excitation Monochromators. Sample compartment is between the two Monochromators where sample is placed. **(Figure 2.5)** The signals generated are detected by detectors. Two detectors are present in a PL device. One is the photon counter the other is reference detector that monitors the light source.

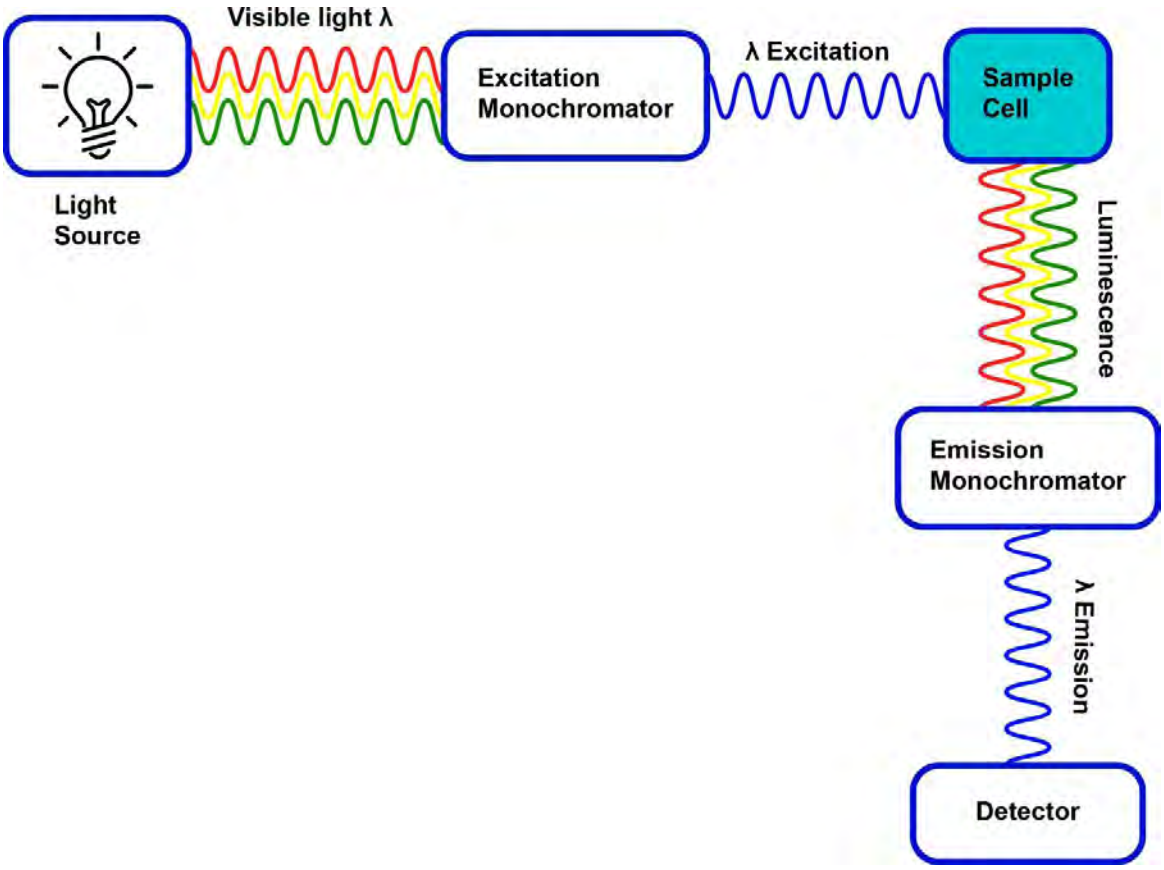

Figure 2.5: Schematic representation of working of photoluminescence.

2.7.2 X-ray diffraction (XRD)

When examining crystals, X-ray diffraction does not do any damage to the sample. Structures, crystal lattice orientation, grain size, structural flaws, etc. are all demonstrated with great precision. If Bragg's law holds true, then X-ray diffraction will occur in the crystal, and we'll be able to learn the d-spacing of the crystal lattice of any crystalline or layered substance

$$n\lambda = 2d\sin\theta$$

Where:

- n= any integer displaying order of diffraction
- λ= wavelength of incident x-ray beam
- d= the spacing between crystal lattice planes
- θ= Bragg's angle of diffraction from different planes

The basic working principle is that diffraction peaks are formed by the constructive interference of a monochrome x-ray beam scattered at a specific angle from each set of lattice planes in a given sample. Following the Scherrer equation, the peak intensities and widths are determined by the atomic distribution within the lattice.

FWHM = (k x λ) / (D x cosθ)

Where:

- FWHM is the full width at half-maximum of the diffraction peak
- K= shape constant
- D= is the crystallite size
- θ = is Bragg's angle of diffraction

Derivation of this equation assumes that each atom scatters the incident x-ray radiations independently, and once scattered the x-ray radiations does not interact with other atoms. Hence the fingerprint of periodic atomic groupings in any particular materials is known as the x-ray diffraction pattern[31]

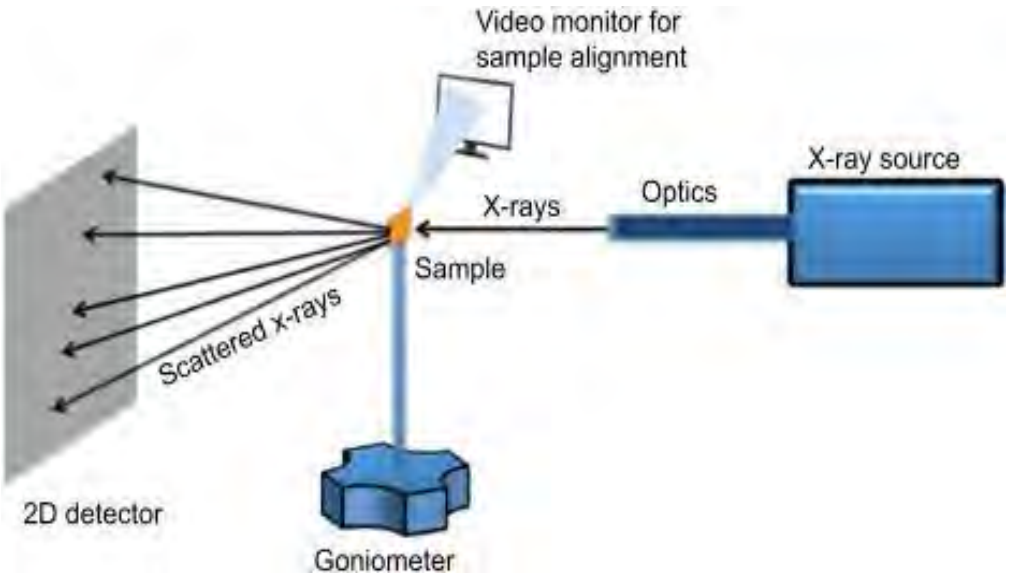

Figure 2.6: Basic instrumentation of x-ray diffraction (XRD) spectroscopy.

2.7.3 Ultraviolet Visible Spectroscopy

Ultraviolet Visible Spectroscopy Ultra-violet visible spectrophotometry is a technique use for measurement of different optical properties of analytes. Ultra-violet visible spectrophotometry is also known as "electronic spectroscopy". It works based on

electromagnetic radiation (EMR), as a result electron of analyte absorb energy and go to excitation state, when the absorb energy release, it irradiates certain types of light with the specific wavelength. UV light has a wavelength range of 190-400 nm, while visible light has a wavelength range of 400-800 nm.

Principle of UV-Visible Spectroscopy

The working principle of UV-Visible spectrophotometer is that when a light beam passes through a material (semiconductor photo catalyst) a wavelength is generated that is specific for certain material. This wavelength reaches the detector where it is measured. This particular wavelength gives specific information the morphology, structure and no of molecules of the element present in the material tested.

When the sample is exposed to light beam, some the light is absorbed by the sample material, rest of the light is transmitted. The ratio between incident light and the transmitted beam gives the value of transmittance. [32]

$T = I/Io$

$T = 10^{-kcl}$

k is proportionality constant & l is the length of light path through the cuvette in cm.

Taking the negative log of transmittance give the value of absorbance.

$Abs = \log (1/T)$

$Abs = \log (Io/I)$

Beer-Lambert Law

There is one specific wavelength at which absorbance value of the material is related directly to the concentration of material and length of path.

$A = \varepsilon cl$

A = absorbance, ε = absorptivity, c = concentration of material and l=length of path[33]

Instrument and working of UV-Visible Spectrophotometer

Following are the main and important components of spectrophotometer.

- A light source (UV and visible region).

- A Monochromators to select wavelength.
- A holder that holds cuvette.
- A wavelength detector
- A readout

The source of UV light is mostly filament of tungsten or sometimes deuterium arc lamp. For visible wavelength, LEDs and xenon lamps are used. Photodiodes are used as detectors. While measuring UV light absorbance, the visible lamp is turned off and vice versa. **(Figure 2.7)**

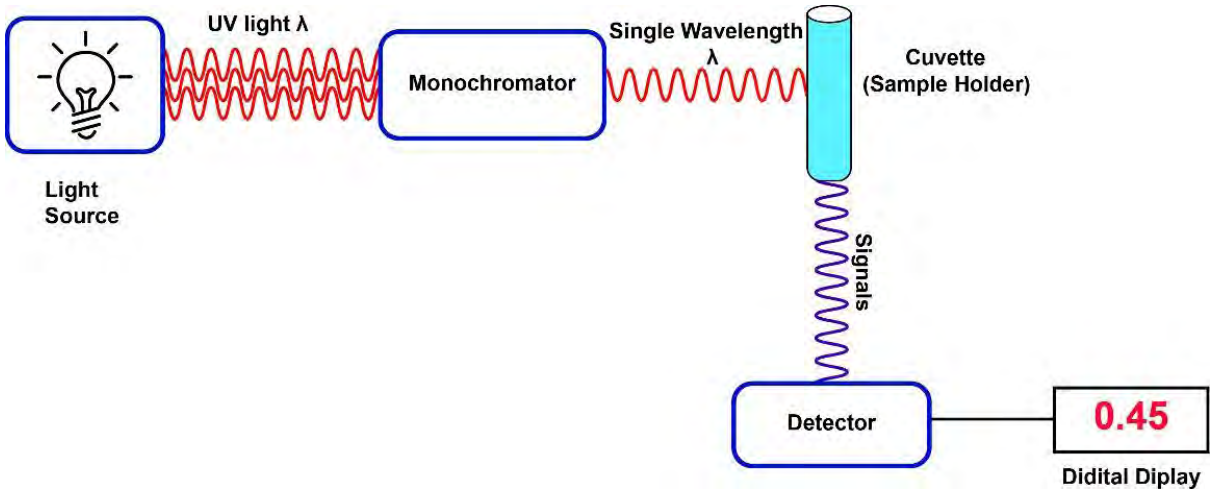

Figure 2.7: Schematic representation of working principle of UV-Visible spectrophotometer.

2.7.4 Scanning Electron Microscopy (SEM)

It is a device in which a high energy electron beam is used for imaging materials to study topography. SEM gives information about surface morphology of material, with in depth focus. It also tells us about material composition [34].

Principle of SEM

It is based on the principle that the primary electrons are emitted by providing energy source to the sample's electrons these electrons are the released as secondary electron. Electromagnetic lenses are used to focus electron beam on the surface of material. The diameter of focused beam is up to 1nm. X-rays Secondary electrons, and backscattered

electrons are produced because of this interaction. These are detected. The number of detected electrons make the image point brighter. SEM has a magnification ranging from 100-1000000X. Magnification can be calculated using following formula:

M = w/l

Where, M is the Magnification, w is width on the screen and l is the scan length on specimen.

Specimen to be observed by SEM must satisfy certain parameters. It must be stable enough to withstand bombardment of high energy electron beams, it must be good conductor of electrons. It must be clean and completely dry.

Instrument of SEM

- The electron source
- Lenses
- Detectors

Electron beam is emitted by the gun that is placed in the vacuum and takes a linear path through electromagnetic lenses and fields. The electron beam is targeted on the sample through an objective lens. The beam of electron will focus the specific region of the sample by using deflector coils which are controlled by scan generator. The size of the pattern is regulated by magnification. **(Figure 2.8)** The magnification adjustments alter the scale of the raster region on the sample [35]. Huge number of signals will be produced when beam of electron strikes with the material i.e., x-rays and electrons are released from the sample. Signals are then detected by the detector and produce signals from where the image will be produced. The signals that have been produced from the sample - electron interaction gives the comprehensive details of the material such as crystalline structure, external morphology, chemical composition and orientation of material.

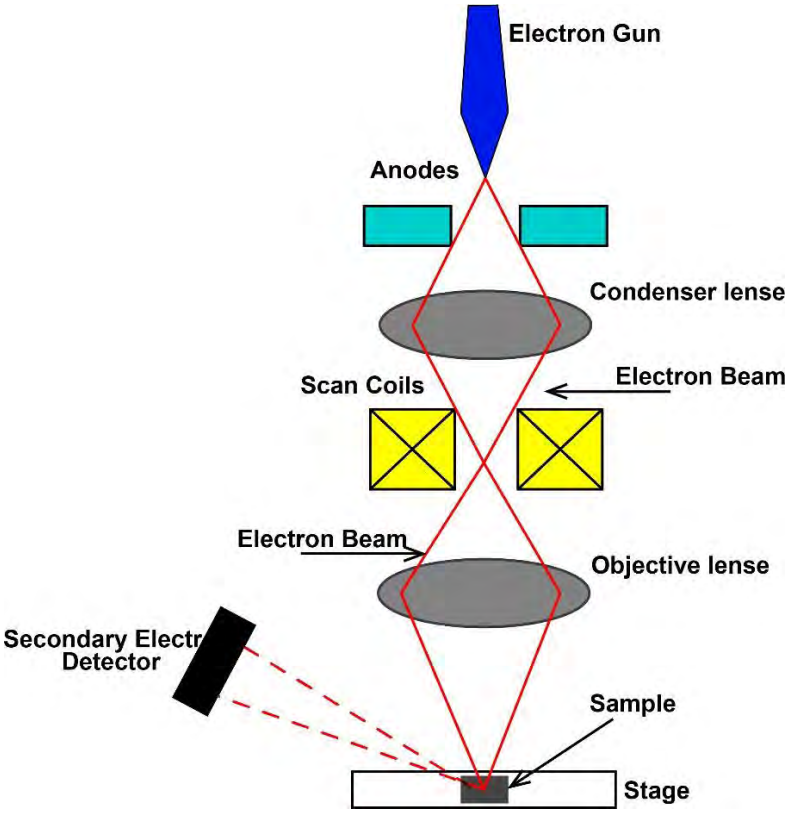

Figure 2.8: Schematic representation of working of SEM.

2.7.5 Transmission Electron Microscopy (TEM)

Transmission electron microscopy is a technology that makes images of nanoparticles using beam of electron. Max Knoll, a German electrical engineer, invented TEM in 1931. When electron passes through the sample, an image is formed on the screen. Transmitted or diffracted electrons are used for TEM imaging [36]

Instrument and working of TEM

Following are the components of TEM.

- Illuminating system
- Objective lenses
- TEM imaging system

Beams of electron emitted from an electron gun could be concentrated by electromagnetic lens that is in the column of TEM and by metal apertures. As the electron being negatively charged particle, they are focused by deflecting toward electric and magnetic field. Electron gun is used to produce a beam of electron and

made fall on the sample by using magnetic condensing lens.[37] The beam will be partially transmitted and partially reflected based on the angle of incidence. Image will be formed on the E-Wald after recombination of these two waves. The combined image is called the contrast image of the process. A contrast in amplitude is obtained that improves the contrast of image. Only with the use of the transmitting beam this can be done and hence the diffracted beam can be eliminated. The resulting beam is now moved through the magnetic objective lens and the aperture to eliminate the diffracted beam. Diffracted image will be eliminated by the adjustment of aperture. Image will be produced only by the transmitted beam alone and is then magnified by passing through the projector lens. Magnified image is then recorded in CCD or fluorescent screen.

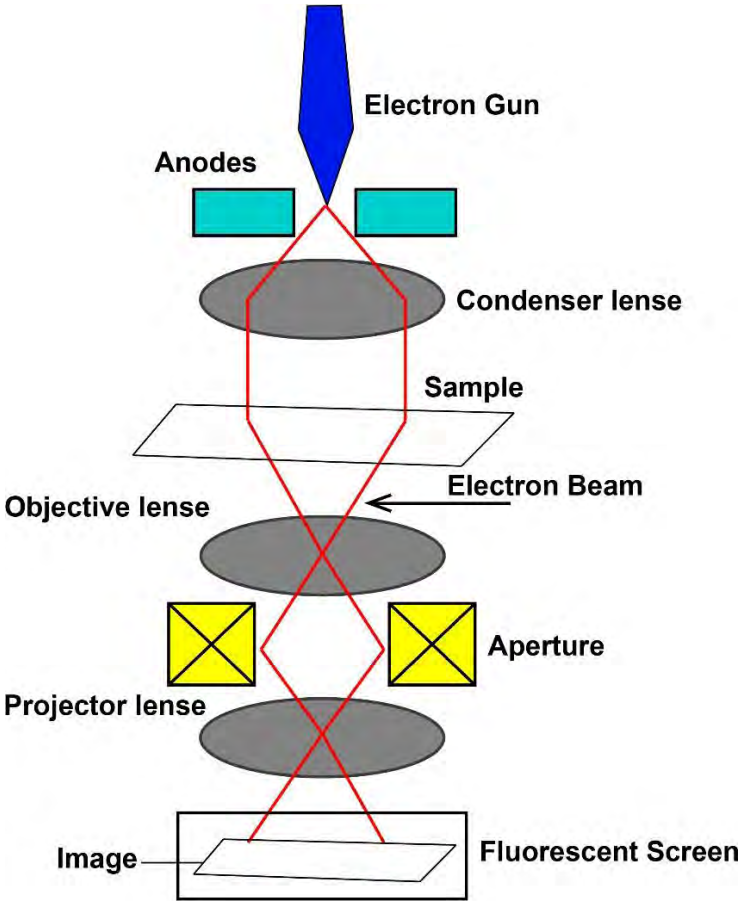

Figure 2.9: Schematic representation of working of TEM.

3. RESULTS AND DISCUSSION

In this chapter, we present the results obtained from a series of experimental and characterization techniques that were used to study the prepared heterostructures of Bi_2O_3, g-C_3N_4, Bi_2O_3/g-C_3N_4, and Co-Bi_2O_3/g-C_3N_4. The samples were characterized by studying their optical properties using a range of different techniques.

A method frequently used to gauge light absorption in the UV-visible portion of the electromagnetic spectrum is UV-DRS (UV Diffuse Reflectance Spectroscopy). This study used it to determine how much light was absorbed by the prepared heterostructures in relation to wavelength. This information was used to determine the bandgap energy of the samples, which is a key parameter for understanding their optical properties.

Scanning electron microscopy (SEM) is a powerful imaging method that shows the surface morphology and structure of materials in high-resolution images. In this study, SEM was used to look at the structure and surface morphology of the heterostructures that had been made, allowing us to gain insight into their physical characteristics and overall structure.

X-ray Diffraction (XRD) is a non-destructive technique that is used to study the crystal structure of materials. It was used in this study to analyze the crystal structure of the prepared heterostructures, including their phase composition, crystal size, and lattice parameters. This information was used to confirm the formation of the desired heterostructure and to identify any potential impurities or defects.

UV-Visible (UV-VIS) spectroscopy is another commonly used technique for studying the optical properties of materials. In this study, UV-VIS spectroscopy was used to measure the absorbance of light by the prepared heterostructures as a function of wavelength. This information was used to determine the optical bandgap of the samples and to identify any potential absorption peaks or spectral features.

Finally, Photoluminescence (PL) spectroscopy is a technique used to study the emission of light from materials that have been excited by light or other energy sources. In this study, PL spectroscopy was used to measure the photoluminescence properties of the prepared heterostructures, providing information on their recombination

dynamics and potential applications in optoelectronics.

In summary, the use of a range of different experimental and characterization techniques allowed us to obtain a comprehensive understanding of the prepared heterostructures of Bi2O3, g-C3N4, Bi2O3/g-C3N4, and Co-Bi2O3/g-C3N4. The results of these analyses are presented in the following sections and provide insights into the potential applications of these materials in various fields, including catalysis, photocatalysis

3.1. Photoluminescence (PL):

To check the recombination process of the photogenerated electron-holes carriers of photocatalyst, photoluminescence (PL) spectra were documented. High intensity of fluorescence encodes high recombination rate of electron-hole pairs thus generating high peaks.[63] **Figure 3.1** presents the PhotoLuminescence spectra of C_3N_4, Bi_2O_3, Bi_2O_3/C_3N_4, and Co-Bi_2O_3/C_3N_4. The peaks show a clear decrease in recombination rate as Bi_2O_3 is treated (doping and heterojunction). This indicates fact that recombination rate of electron-hole pairs is high in pure C_3N_4. A sharp decrease in recombination rate can be observed in **Co-Bi_2O_3/C_3N_4** compared to others. The order of recombination rate is **C_3N_4 > Bi_2O_3 > Bi_2O_3/C_3N_4 > Co Bi_2O_3/C_3N_4.**

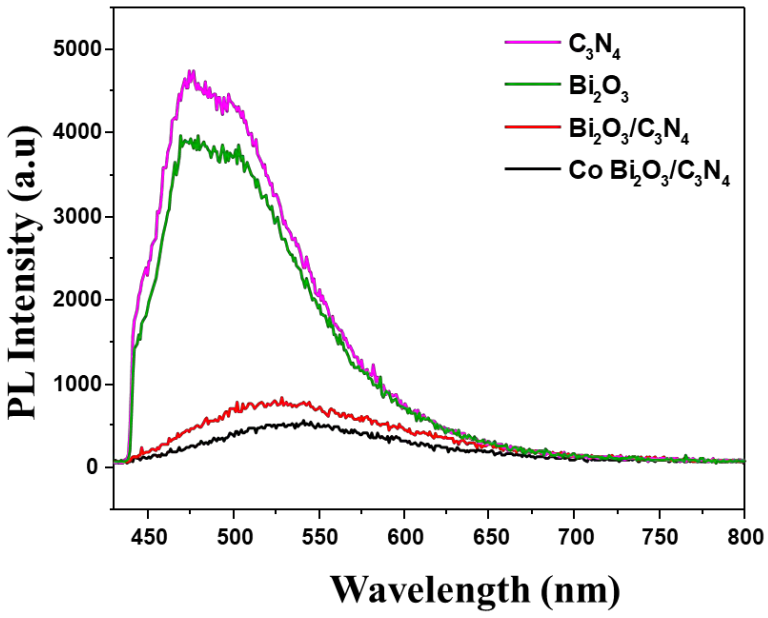

Figure 3.1: Photoluminescence (PL) spectrum of as prepared samples of C_3N_4, Bi_2O_3, Bi_2O_3/C_3N_4, and Co-Bi_2O_3/C_3N_4

3.2. UV-Vis DRS Analysis

Figure 3.2 presents the UV-DRS spectra for all the samples. The band-gap values were calculated using the UV-DRS spectra. Differences in morphology, as well as the band-gap of the as synthesized samples, revealed a band-gap in the visible region of the electromagnetic spectrum [38]. The prepared heterojunction nearly absorbed all light in the wavelength region of 350 to 700 nm, which means that as prepared heterojunction are visible light active. Figure 3.2 shows that Co-Bi2O3/g-C3N4 has lower band gap than pure bismuth. This confirms that metal doping has tailored theband gap of pure bismuth. Its energy gap may change from about 2 to 3.96 eV[39]

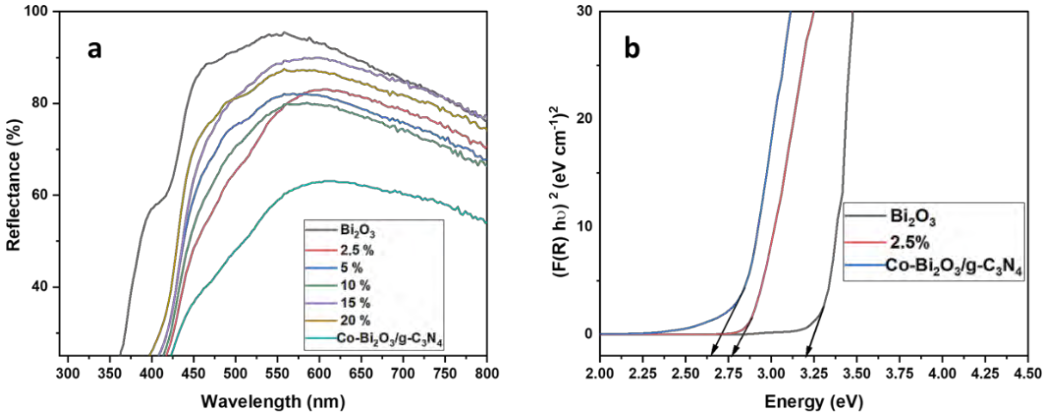

Figure 3.2: (a) UV-visible diffuse reflectance spectra (DRS) of synthesized samples. (b) Band gap diagram of synthesized samples.

3.3. Scanning electron microscopy

The powerful imaging technique known as scanning electron microscopy (SEM) provides high-resolution images of the surface morphology and structure of materials. In the present investigation, a scanning electron microscope (SEM) was utilized to investigate the morphology of the prepared photocatalysts. According to the findings, the morphology of Bi_2O_3 is a regular spheroidal structure with a mean size of about 0.5-2 micrometers. In contrast, pure g-C_3N_4 has aggregated morphologies composed of block-based flakiness and particles.. This is consistent with previous studies on the morphology of g-C_3N_4, which has been found to exhibit complex structures due to its layered stacking and intermolecular forces.

The Co-Bi_2O_3/g-C_3N_4 sample, however, exhibits a significant change in morphology compared to the individual components. The morphology shows many aggregated flakiness, which suggests that the cobalt and bismuth have been aggregated on the surface of g-C_3N_4. This is a promising result, as the aggregation of these metals on the surface of the g-C_3N_4 can enhance the photocatalytic activity of the heterojunction.

The observed changes in morphology in the as-synthesized heterojunction can be attributed to the interaction between the different materials during the preparation process. The strong interaction between Bi_2O_3 and g-C_3N_4 can lead to the formation of a hybrid structure that combines the advantages of both materials. The addition of Co-Bi_2O_3 further modifies the structure and enhances the photocatalytic activity of the heterojunction.

Overall, the use of SEM allowed us to gain valuable insights into the morphology and structure of the prepared photocatalysts, which can help to inform the design and optimization of these materials for various applications

.

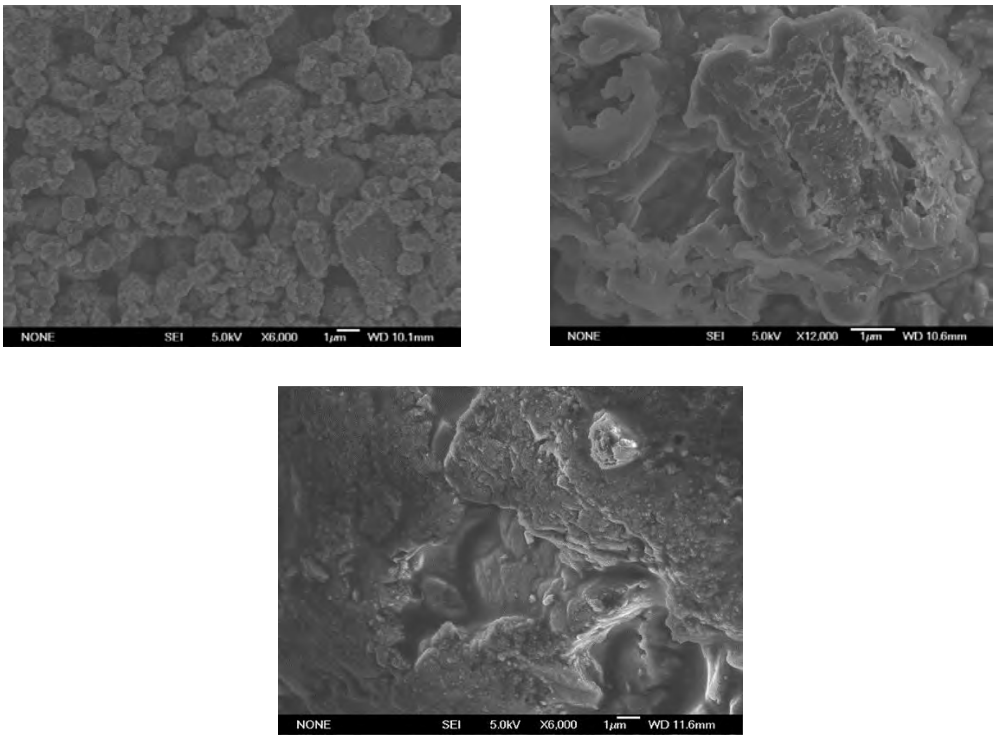

Figure 3.3: SEM images of C_3N_4, Bi_2O_3 and Co-Bi_2O_3/g-C_3N_4.

3.4.X-Ray Diffraction (XRD)

All samples' phase structures were determined using XRD. Pure g-C_3N_4 has two separate diffraction peaks at 13.7° and 27.4°, corresponding to the (100) and (002) crystal planes of

g-C_3N_4, respectively. Pure Bi_2O_3 has high crystallinity, and all diffraction peaks can be classified as monoclinic. Bi_2O_3 diffraction peaks are assigned to the crystal planes (102), (122), and (200) of Bi_2O_3.

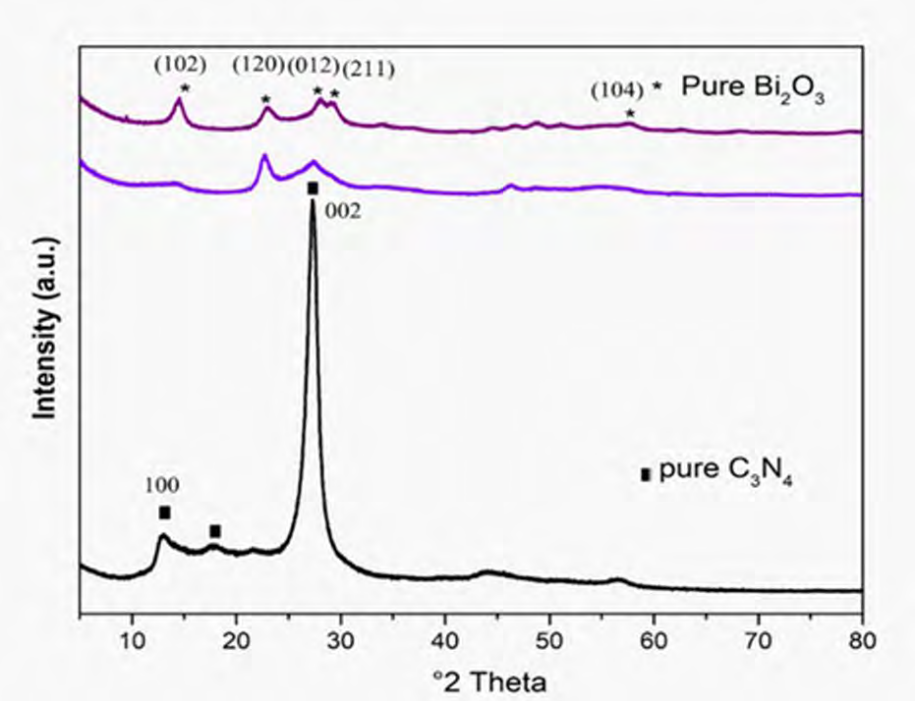

Figure 3.4: XRD pattern of C_3N_4, Bi_2O_3 and Co-Bi_2O_3/g-C_3N_4.

3.5.Photocatalytic activity test

Photocatalytic activity was evaluated by degrading 4-Nitrophenol in natural sunlight. All eight samples i.e., g-C_3N_4, Bi_2O_3, 2.5% Bi_2O_3/g-C_3N_4, 5% Bi_2O_3/g-C_3N_4, 10% Bi_2O_3/g-C_3N_4, 15% Bi_2O_3/g-C_3N_4, 20% Bi_2O_3/g-C_3N_4 were tested in direct sunlight with lux of 120,000 lux. 4 nitro phenol pure crystals was used as pollutant. 50ml of stock solution of 4 NP was taken in eight separate beakers. Beakers were tagged by catalysts names i.e., g-C_3N_4, Bi_2O_3, 2.5% Bi_2O_3/g-C_3N_4 , 5% Bi_2O_3/g-C_3N_4, 10% Bi_2-O3/g-C3N_4, 15% Bi_2O_3/g-C_3N_4, 20% Bi_2O_3/ g-C_3N_4 and Co-Bi_2O_3/g-C_3N_4 .Samples of pure pollutant were taken. 10mg of each of the four catalysts were added in respective beakers and kept in dark for 30 minutes to attain absorbance equilibrium. Then the same solutions were placed in open air with continuous stirring. Samples were taken after every 30 minutes. After 2 hours reaction, all the samples were centrifuged. UV-Visible

spectrum was calculated. Figure 3.5 a, b, c, and d shows absorbance spectra of g-C_3N_4, Bi_2O_3, 2.5% Bi_2O_3/g-C_3N_4, and Co-Bi_2O_3/g-C_3N_4 respectively.

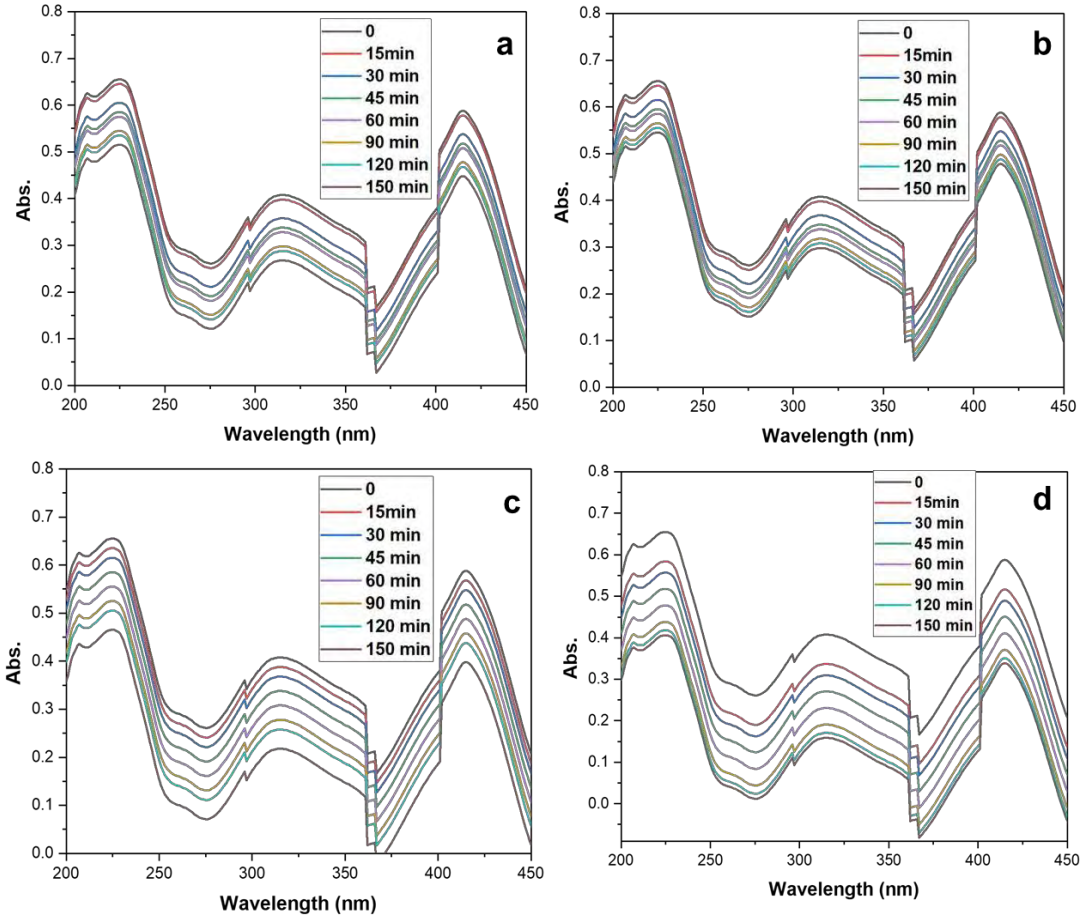

Figure 3.5: UV-Vis absorbance spectra of 4-Nitrophenol in 150 minutes using (a)g-C_3N_4, (b)Bi_2O_3, (c) 2.5 % Bi_2O_3/g-C_3N_4, (d) Co-Bi_2O_3/g-C_3N_4.

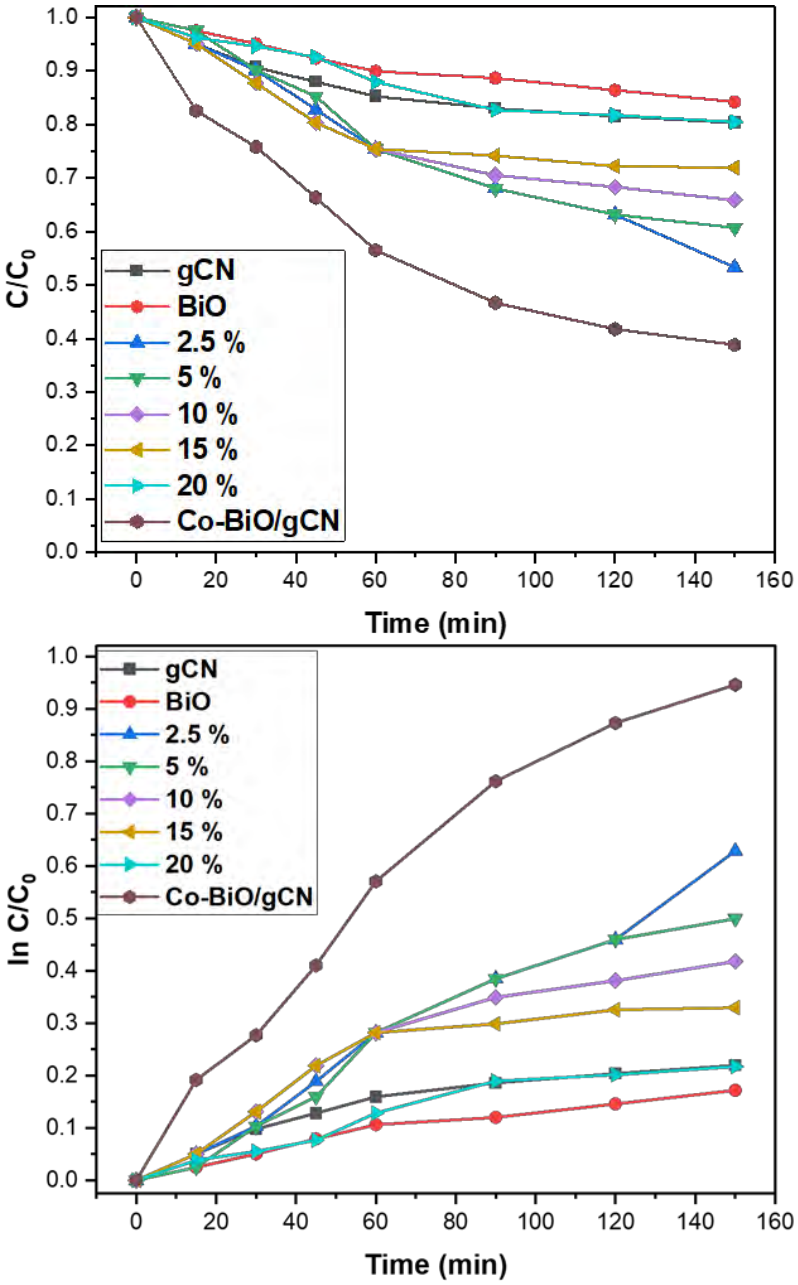

,

Figure 3.6: (a) C/C_0 vs Time (min) (b) $-\ln(C/C_0)$ vs Time plot

$C(t) = C_0e^{(-kt)}$. Where k_t is molar distinction coefficient. Rate of degradation k/min is the value of slope obtained from $-\ln(C/C_0)$ vs time plot. k/min values of all the eight samples are given in **Table 3.1**. This shows that Co-Bi_2O_3/g-C_3N_4 has maximum degradation rate.

Table 3.1: Overall kinetics of photocatalytic degradation of 4-Nitrophenol under solar light

Photocatalysts	Degradation rate k/min	Adj. R-square	Percentage Degradation
Co-Bi_2O_3/ g-C_3N_4	$0.00389 \pm 5.15*10^{-4}$	0.874	61
g-C_3N_4	$0.00122 \pm 2.04*10^{-4}$	0.832	19.7
Bi_2O_3	$0.00102 \pm 1.06*10^{-4}$	0.932	15.7
2.5 %	$0.00309 \pm 1.83*10^{-4}$	0.975	46.6
5 %	$0.00285 \pm 2.90*10^{-4}$	0.931	39.3
10 %	$0.00228 \pm 3.93*10^{-4}$	0.863	34.1
15 %	$0.00184 \pm 3.92*10^{-4}$	0.750	28
20 %	$0.00138 \pm 1.49*10^{-4}$	0.920	19

3.6.Percentage Degradation

Figure 3.6 shows percentage degradation of 4-Nitrophenol using all different catalysts. It is very clear that Co- Bi_2O_3/ gC_3N_4 has degraded 4-Nitrophenol up to 61 % in 150 minutes. 2.5% Bi_2O_3/ gC_3N_4 has degraded up to 46.6 % in 150 minutes. The photocatalytic activity of a sample gradually decreases as its Bi_2O_3 concentration increases. Bi_2O_3 has a significant impact on the photocatalytic activity of samples, as is evident. Although the addition of Bi_2O_3 may increase photocatalytic activity, but the levels of photocatalytic activity vary. The reason may be that when the Bi_2O_3 concentration exceeds 2.5%, the surface of gC_3N_4 is coated with Bi_2O_3 powder, which inhibits light absorption and reduces the rate of photoexcited charge carrier generation. Under experimental conditions, 2.5% is the optimal Bi_2O_3 concentration in Bi_2O_3/gC_3N_4 samples.

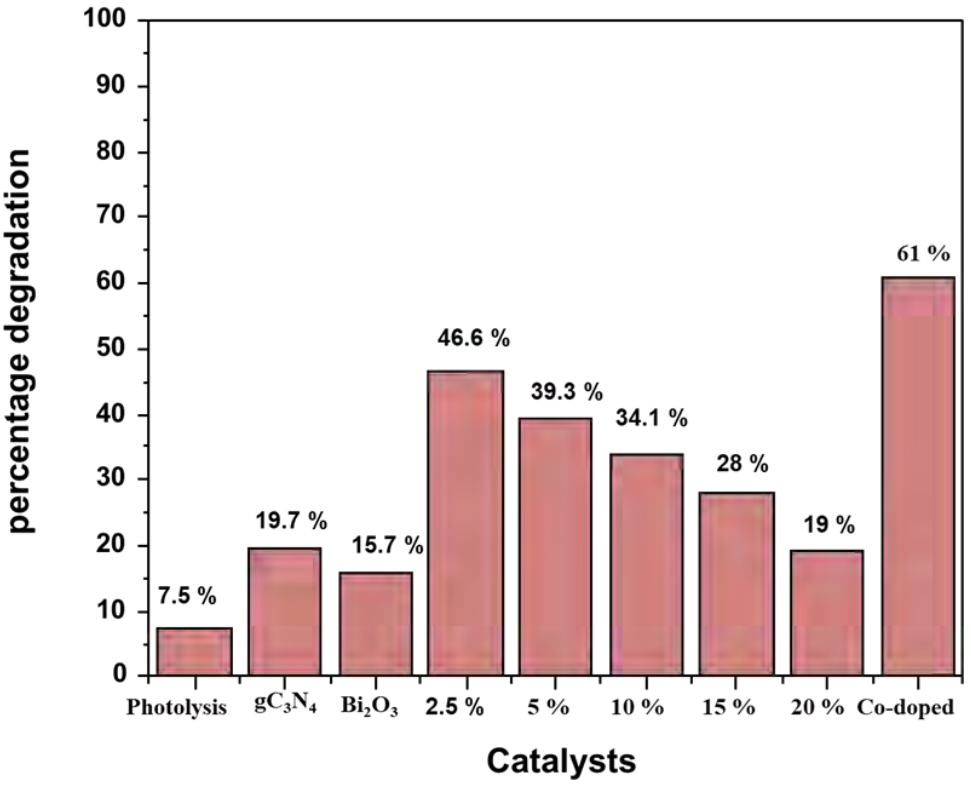

Figure 3.6: Percentage degradation of 4-Nitrophenol using all the catalysts.

3.7.Adsorption Reaction

Adsorption Capacity of four catalyst i.e., g-C_3N_4, Bi_2O_3, 2,5% Bi_2O_3/g-C_3N_4, and Co-Bi_2O_3/g-C_3N_4. Reaction was carried out under the absence of any kind of light. Solution was under continuous stirring. Reaction conditions were kept same. Figure 3.7 shows the C/C_o Vs time graph of all the catalysts. Co-Bi_2O_3/g-C_3N_4 showed the maximum degradation still less than 10 %. This means that catalysts andheterojunctions are activated by visible light and inactive in dark.

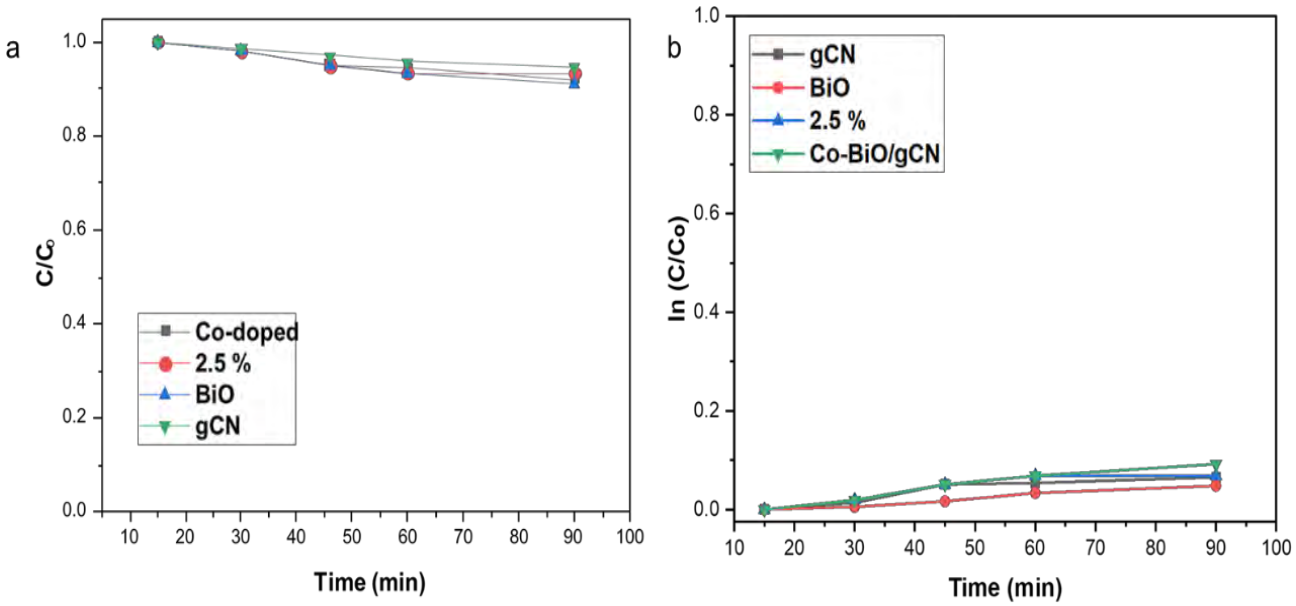

Figure 3.7: (a) C/C_0 graph of adsorption reaction (b) ln C/C_0 of adsorption reaction

3.8.Effect of photolysis

The process of natural degradation of 4-nitrophenol was studied before looking at the role of photocatalyst in its destruction. For that purpose 4-Nitrophenol solution was kept in solar light irradiation for 150 minutes. Negligible photolysis was observed in the absence of any catalyst.

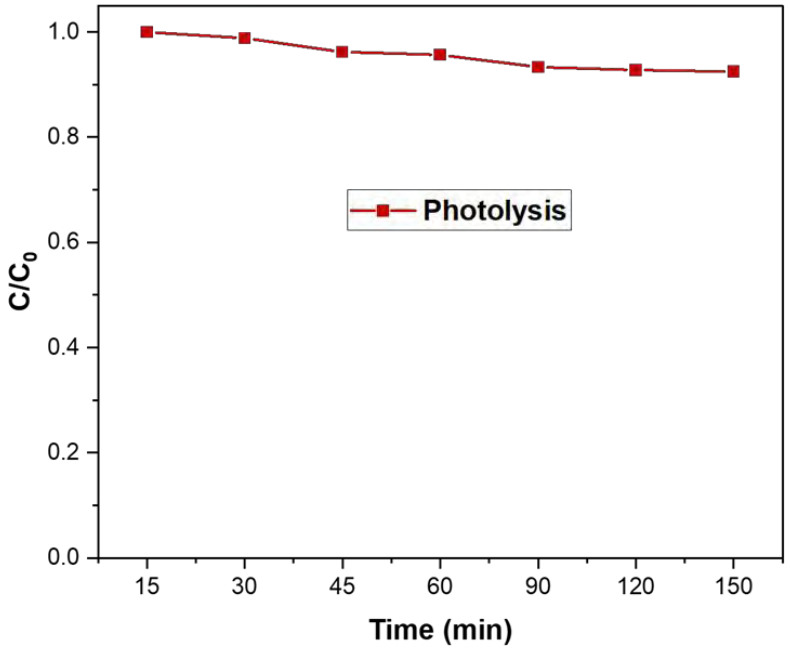

Figure 3.8: Effect of photolysis

3.9. Effect of Catalyst amount at degradation of 4-Nitrophenol:

Different amount of catalyst concentrations has different rate of degradation. Reaction kinetics was checked at 4 different doses of catalyst i.e, 0.1 g/L, 0.15 g/L, 0.2 g/L, 0.3m g/L. Highest degradation rate was observed at 0.2 g/L that was 75% followed by 0.15 g/L degradation percent was 66 % and then 0.3 g/L which was 63% while 0.1 g/L showed lowest degradation rate which was 61%. It is concluded from the given figure 3.8 that the highest degradation was occurred while using 0.2 g/L dose of catalyst, as the concentration of catalyst increased up to 0.3g/L then it was observed that, due to shadow effects of catalyst the rate of degradation declined.

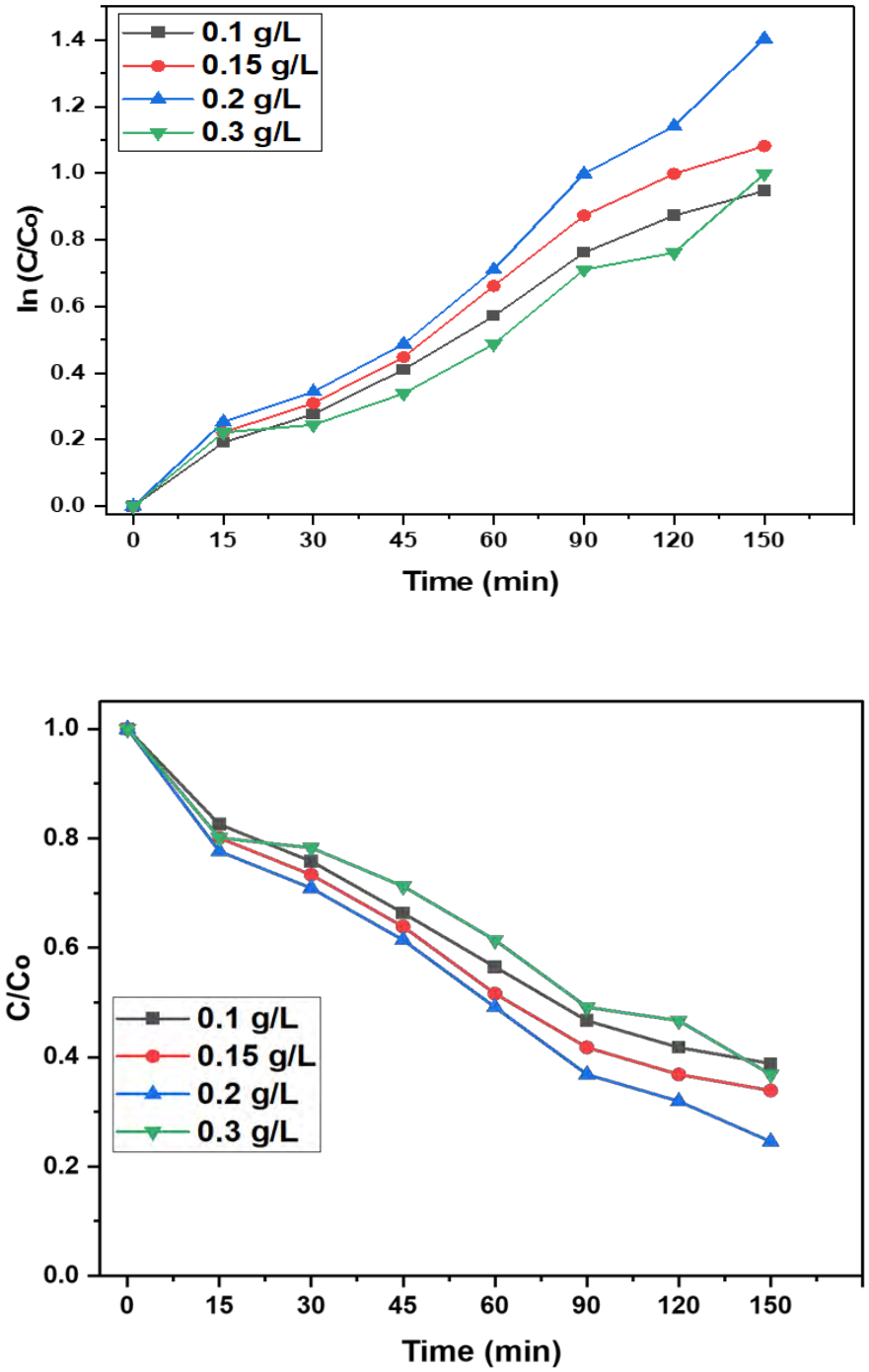

Figure 3.9: (a)Effect of different doses of catalyst on the rate degradation of 4-Nitrophenol (b) ln C/C_o versus time plot

3.10. Effect of concentration of pollutant on degradation of 4-Nitrophenol:

Different amount of initial pollutant concentrations has different rate of degradation. Reaction kinetics was checked at 4 different initial concentrations of 4-Nitrophenol i.e, 10ppm 15ppm, 20ppm and 25ppm. Highest degradation rate was observed at 10ppm pollutant concentration that was 61% followed by 15 ppm and degradation percent was 55% and then 0.3 g/L which was 63% while 0.1 g/L showed lowest degradation rate which was 61%. It is concluded from the given figure 3.10 that the highest degradation was occurred when the initial concentration of pollutant was 10ppm and lowest degradation was observed when th e initial concentarion of 4-Nitrophenol was 25ppm.

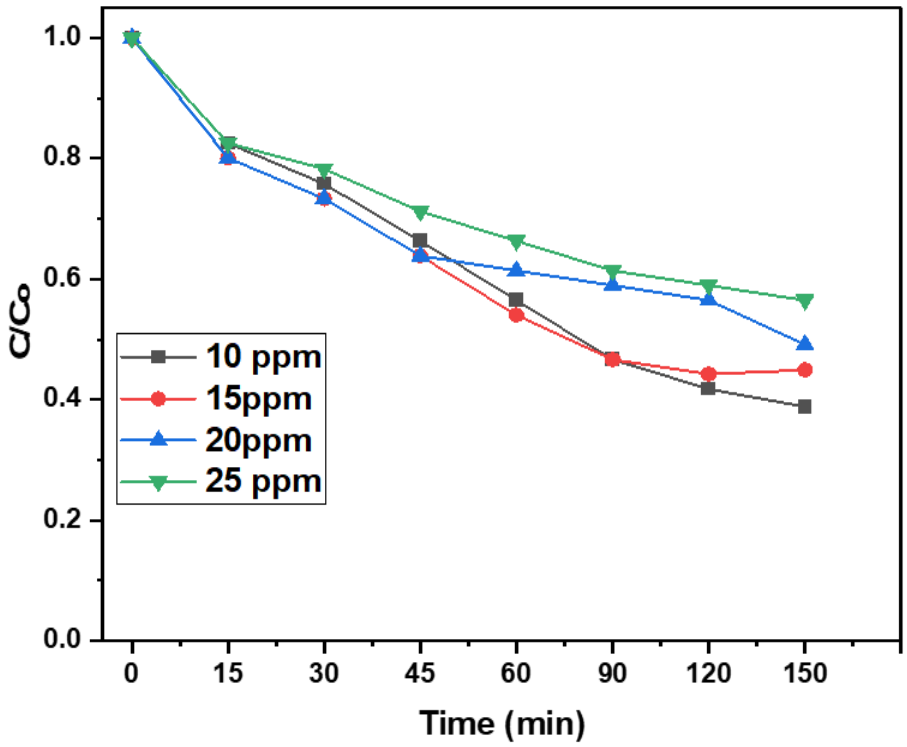

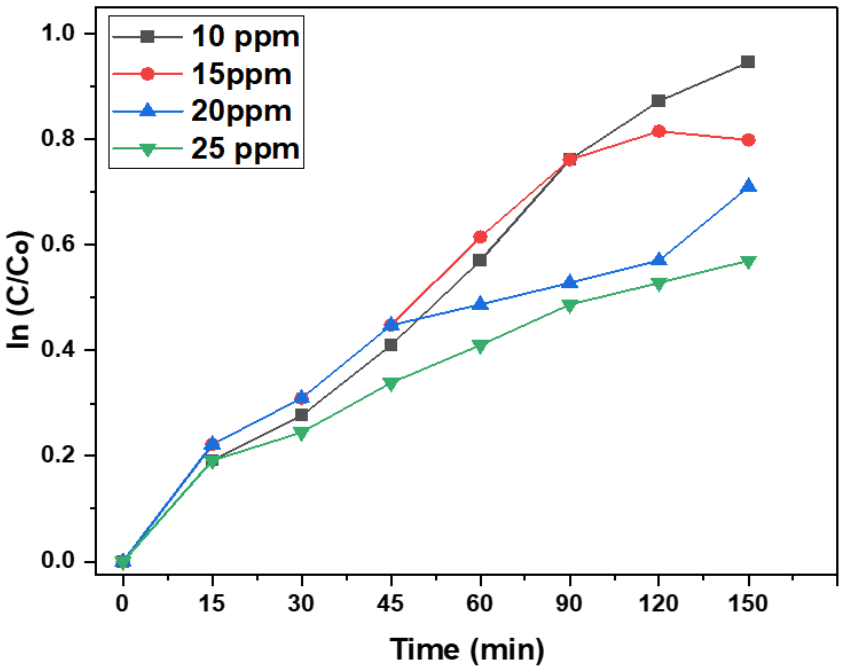

Figure 3.10: (a)Effect of different initial concentration of pollutant on the rate degradation of 4-Nitrophenol (b) ln C/C_o versus time plot

3.11. Effect of pH at degradation of 4-Nitrophenol

4-Nitrophenol was degraded in acidic pH. Effect of different pH were checked to calculate the efficiency of catalyst Co-Bi_2O_3/g-C_3N_4 to degrade levofloxacin. pH of solutions was adjusted by 0.1N of HCl and NaOH which were so diluted. And also, it has no effects on the catalyst structure. The results are shown in figure 3.11 and can be clearly seen that highest degradation was observed in pH 3 which was 80% while pH 5 and pH 7 were observed low-rate degradation that were 75% and 61% respectively.

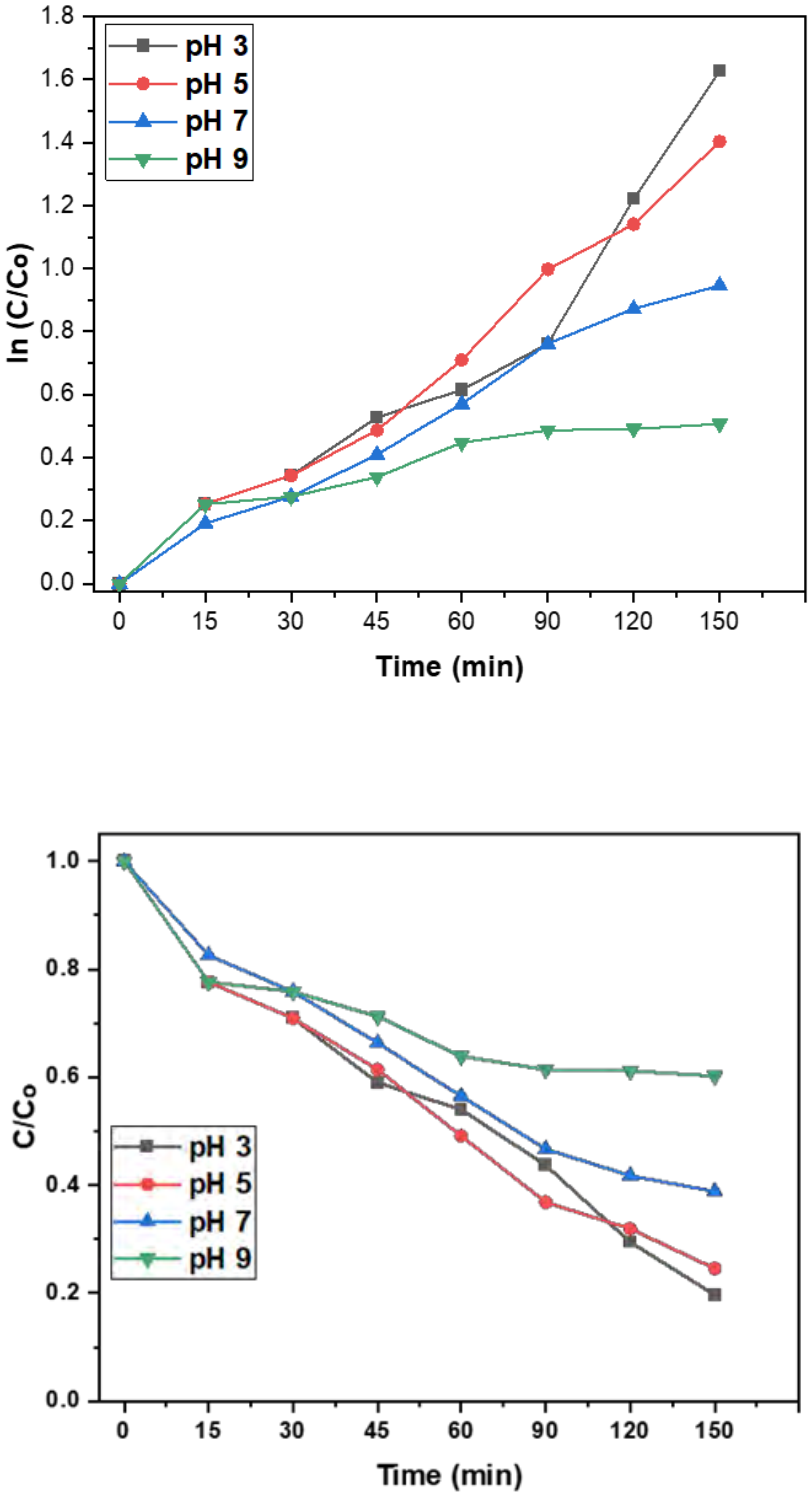

Figure 3.11: (a)Effect of different pH on the rate degradation of 4-Nitrophenol (b) ln C/C_o versus time plot

3.7. Proposed Mechanism

On the basis of the results of structure characterizations and photocatalytic tests, it is possible to propose a mechanism for the enhanced visible light photocatalytic performance of a Bi_2O_3/g-C_3N_4 composite in the degradation of 4-nitrophenol. The formation of an interfacial heterojunction structure is facilitated by the strong interaction between Bi_2O_3 and g-C_3N_4. [40]. Because g-C_3N_4 and Bi_2O_3 have a narrow band gap, their valence band electrons can be excited into their conduction bands when exposed to light, resulting in the formation of photo-induced holes in their valence bands. [41]. The electron-hole separation process of the Bi_2O_3/g-C_3N_4 composite differs from that of conventional composite photocatalysts. In this composite, the interfacial heterojunction structure enables a Z-scheme mechanism in which photo-generated electrons from the conduction band of Bi_2O_3 can efficiently transfer to the valence band of g-C_3N_4 and recombine with holes. Holes in the valence band of Bi_2O_3 can simultaneously oxidize 4-Nitrophenol by reacting with H_2O or with OH radicals produced from water. This occurs because Bi_2O_3 has a more positive EVB than $\cdot OH/OH$ (+1.99 eV vs. NHE, 3.13 eV). [42][43] Furthermore, the electrons in the CB of g-C_3N_4 may reduce molecular oxygen to produce, as its ECB (1.12 eV vs. NHE) is more negative than that of $O_2/\cdot O_2$ (0.33 eV vs. NHE). Both the oxygen and hydrogen peroxide radicals are capable of oxidizing 4-nitrophenol. As a result, both hydroxyl and superoxide radicals are capable of destroying 4-Nitrophenol. [44]

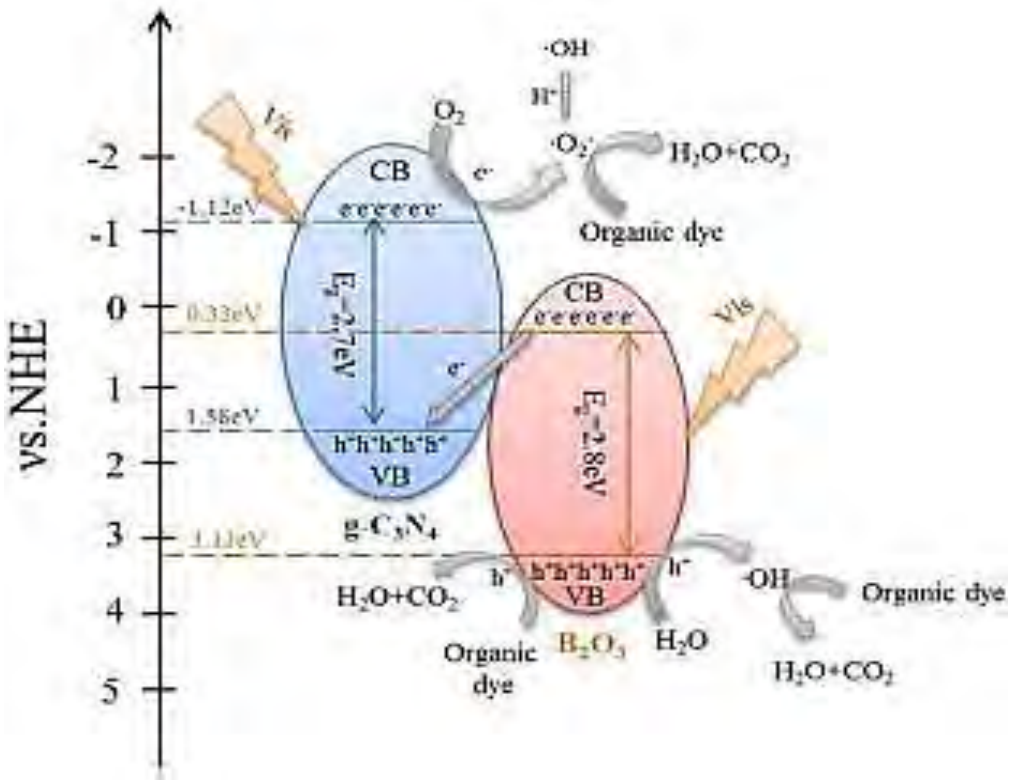

Figure 3.8: Proposed mechanism of Bi_2O_3/g-C_3N_4 photocatalyst[40].

4. CONCLUSION

This study describes the successful thermal synthesis of eight visible light active photocatalysts, including g-C_3N_4, Bi_2O_3, 2.5% Bi_2O_3/g-C_3N_4, 5% Bi_2O_3/g-C_3N_4, 10% Bi_2O_3/g-C_3N_4, 15% Bi_2O_3/g-C_3N_4, 20% Bi_2O_3/g-C_3N_4, and Co-Bi_2O_3/g-C_3N_4. In visible light, the Co-Bi_2O_3/g-C_3N_4 heterojunction exhibited greater degradation efficiency than bare Bi_2O_3, g-C_3N_4, and Bi_2O_3/g-C_3N_4. This heterojunction method shows that the resulting heterostructures exhibit high visible region absorption and increased photodegradation of 4-nitrophenol. Co-Bi_2O_3/g-C_3N_4 heterojunction under visible light for 150 minutes resulted in the greatest 4-nitrophenol degradation rate. Several characterisation techniques, including Photoluminisce, Ultraviolet Diffuse Reflectance Spectroscopy, and X-ray Diaffration, were applied in order to validate the successful creation of hetrojuction. The results reveal that Co-Bi_2O_3/C_3N_4 was successfully synthesized. The investigation confirms that heterojunction Co-Bi_2O_3/g-C_3N_4 as produced is an efficient and effective photocatalyst for the successful degradation of 4-nitrophenol**.**

5. References

[1] K. Kumar Jaiswal, C. R. Chowdhury, D. Yadav, R. Verma, S. Dutta, K. S. Jaiswal, Sangmesh, K. K. SelvaKumar, *Energy Nexus* **2022**, 100118.

[2] B. K. Biswas, *Emerg. Issues Clim. Smart Livest. Prod.* **2022**, 263–316.

[3] R. Chormare, M. A. Kumar, *Chemosphere* **2022**, *302*, 134836.

[4] P. Sharma, J. Prakash, R. Kaushal, *Environ. Res.* **2022**, *212*, 113328.

[5] I. Othman, J. Hisham Zain, M. Abu Haija, F. Banat, *Appl. Catal. B Environ.* **2020**, *266*, 118601.

[6] X. Duan, F. Ma, Z. Yuan, X. Jin, L. Chang, *J. Taiwan Inst. Chem. Eng.* **2013**, *44*, 95–102.

[7] W. W. Anku, M. A. Mamo, M. A. Mamo, P. W. Penny, P. P. Govender, *Phenolic Compd. Nat. Sources, Importance Appl.* **2017**, 419–443.

[8] J. P. Kulkarni, Sunil J and Kaware, *Int. J. Sci. Res. Publ.* **2013**, *3*, 1–5.

[9] B. Zhao, G. Mele, I. Pio, J. Li, L. Palmisano, G. Vasapollo, *J. Hazard. Mater.* **2010**, *176*, 569–574.

[10] Y. Fan, D. Wu, S. Zhang, L. Zhang, W. Hu, C. Zhu, X. Gong, *Green Chem. Eng.* **2022**, *3*, 15–24.

[11] M. R, J. R. J. UC, D. Pinheiro, S. Devi KR, *Appl. Surf. Sci. Adv.* **2022**, *10*, 100265.

[12] A. Aleboyeh, H. Aleboyeh, Y. Moussa, *Dye. Pigment.* **2003**, *57*, 67–75.

[13] M. Achparaki, E. Thessalonikeos, H. Tsoukali, O. Mastrogianni, E. Zaggelidou, F. Chatzinikolaou, N. Vasilliades, N. Raikos, M. Isabirye, D. V. . Raju, M. Kitutu, V. Yemeline, J. Deckers, J. Poesen Additional, *Intech* **2012**, 13.

[14] N. Schweigert[2], A. J. B. Zehnder, R. I. L. Eggen, *Chemical Properties of*

Catechols and Their Molecular Modes of Toxic Action in Cells, from Microorganisms to Mammals, **2001**.

[15] J. A. Garrido-Cardenas, B. Esteban-García, A. Agüera, J. Antonio Sánchez-Pérez, F. Manzano-Agugliaro, **n.d.**, DOI 10.3390/ijerph17010170.

[16] J. J. Pignatello, E. Oliveros, A. MacKay, *Crit. Rev. Environ. Sci. Technol.* **2006**, *36*, 1–84.

[17] G. H. Sonawane, S. P. Patil, S. H. Sonawane, *Appl. Nanomater.* **2018**, 1–22.

[18] A. Nickheslat, M. M. Amin, H. Izanloo, A. Fatehizadeh, S. M. Mousavi, *J. Environ. Public Health* **2013**, *2013*, DOI 10.1155/2013/815310.

[19] M. A. Rauf, S. S. Ashraf, *Chem. Eng. J.* **2009**, *151*, 10–18.

[20] G. Viruthagiri, P. Kannan, *J. Mater. Res. Technol.* **2019**, *8*, 127–133.

[21] H. Chen, C. Yu, Z. Xue, P. Wang, Z. Wang, Q. Cong, L. Pei, C. Fan, *Toxicol. Environ. Chem.* **2020**, *102*, 356–385.

[22] J. Zhang, Y. Hu, X. Jiang, S. Chen, S. Meng, *J. Hazard. Mater.* **2014**, *280*, 713–722.

[23] J. Zhang, Y. Hu, X. Jiang, S. Chen, S. Meng, X. Fu, *J. Hazard. Mater.* **2014**, *280*, 713–722.

[24] S. Liu, J. Chen, D. Xu, X. Zhang, M. Shen, *J. Mater. Res.* **2018**, *33*, 1391–1400.

[25] M. Zhou, H. Ou, S. Li, X. Qin, Y. Fang, S.-C. Lee, X. Wang, W. Ho, **2021**, DOI 10.1002/advs.202102376.

[26] V. Yadav, P. Verma, H. Sharma, S. Tripathy, V. K. Saini, *Environ. Sci. Pollut. Res.* **2020**, *27*, 10966–10980.

[27] D. Titus, E. James Jebaseelan Samuel, S. M. Roopan, *Green Synth. Charact. Appl. Nanoparticles* **2019**, 303–319.

[28] M. Manso, M. L. Carvalho, *Spectrochim. Acta Part B At. Spectrosc.* **2009**, *64*, 482–490.

[29] V. Singh, P. Yadav, V. Mishra, *Green Synth. Nanomater. Bioenergy Appl.* **2020**, 83–97.

[30] S. Eaton-Magaña, C. M. Breeding, *GEMS Gemol.* **2016**, *52*, 2–17.

[31] F. T. L. Muniz, M. A. R. Miranda, C. Morilla Dos Santos, J. M. Sasaki, *Acta Crystallogr. Sect. A Found. Adv.* **2016**, *72*, 385–390.

[32] J. S. Zavahir, Y. Nolvachai, P. J. Marriott, *TrAC - Trends Anal. Chem.* **2018**, *99*, 47–65.

[33] A. K. Tiwari, A. Kumar, Z. Said, *Adv. Nanofluid Heat Transf.* **2022**, 59–93.

[34] **2014**, DOI 10.1007/978-3-662-53120-4.

[35] T. L. Hayes, R. F. Pease, *The Scanning Electron Microscope: Principles and Applications in Biology and Medicine.*, ACADEMIC PRESS, INC., **1968**.

[36] S. Casciardi, R. Sisto, M. Diociaiuti, *J. Nanomater.* **2013**, *2013*, 15.

[37] H. Ma, K.-J. Shieh, T. X. Qiano, *Nat. Sci.* **2006**, *4*, 14–22.

[38] W. Avansi, V. R. De Mendonça, O. F. Lopes, C. Ribeiro, *RSC Adv.* **2015**, *5*, 12000–12006.

[39] L. Leontie, M. Caraman, A. Visinoiu, G. I. Rusu, *Thin Solid Films* **2005**, *473*, 230–235.

[40] Y. Cui, X. Zhang, R. Guo, H. Zhang, B. Li, M. Xie, Q. Cheng, X. Cheng, *Sep. Purif. Technol.* **2018**, *203*, 301–309.

[41] E. J. Li, K. Xia, S. F. Yin, W. L. Dai, S. L. Luo, C. T. Au, *Mater. Chem. Phys.* **2011**, *125*, 236–241.

[42] S. Chen, Y. Hu, S. Meng, X. Fu, *Appl. Catal. B Environ.* **2014**, *150–151*, 564–573.

[43] W. Li, D. Li, Y. Lin, P. Wang, W. Chen, X. Fu, Y. Shao, *J. Phys. Chem. C* **2012**, *116*, 3552–3560.

[44] Y. Lin, D. Li, J. Hu, G. Xiao, J. Wang, W. Li, X. Fu, *J. Phys. Chem. C* **2012**,

116, 5764–5772.

[45] S. Dalal, R. R. Pandey, R. C. Dubey, *Bioremediation Pollut.* **2012**, 1–23.

Hajra Batool

ORIGINALITY REPORT

16%	5%	12%	5%
SIMILARITY INDEX	INTERNET SOURCES	PUBLICATIONS	STUDENT PAPERS

PRIMARY SOURCES

1	Wee-Jun Ong, Lling-Lling Tan, Yun Hau Ng, Siek-Ting Yong, Siang-Piao Chai. " Graphitic Carbon Nitride (g-C N)-Based Photocatalysts for Artificial Photosynthesis and Environmental Remediation: Are We a Step Closer To Achieving Sustainability? ", Chemical Reviews, 2016 Publication	2%
2	Zhang, Jinfeng, Yingfei Hu, Xiaoliang Jiang, Shifu Chen, Sugang Meng, and Xianliang Fu. "Design of a direct Z-scheme photocatalyst: Preparation and characterization of Bi2O3/g-C3N4 with high visible light activity", Journal of Hazardous Materials, 2014. Publication	1%
3	William W. Anku, Messai A. Mamo, Penny P. Govender. "Chapter 17 Phenolic Compounds in Water: Sources, Reactivity, Toxicity and Treatment Methods", IntechOpen, 2017 Publication	1%